Transform Migration and Vertical Tectonics at the Romanche Fracture Zone, Equatorial Atlantic

Article *in* Journal of Geophysical Research Atmospheres · November 1994

DOI: 10.1029/94JB01178

JOURNAL OF GEOPHYSICAL RESEARCH, VOL. 99, NO. B11, PAGES 21,779–21,802, NOVEMBER 10, 1994

Transform migration and vertical tectonics at the Romanche fracture zone, equatorial Atlantic

E. Bonatti,[1] M. Ligi,[2] L. Gasperini,[2] A. Peyve,[3] Y. Raznitsin,[3] and Y. J. Chen[4]

Abstract. The Romanche transform offsets the Mid-Atlantic Ridge (MAR) axis by about 950 km in the equatorial Atlantic. Multibeam and high-resolution multichannel seismic reflection surveys as well as rock sampling were carried out on the eastern part of the transform with the R/V *Akademik Strakhov* as part of the Russian-Italian Mid-Atlantic Ridge Project (PRIMAR). Morphobathymetric data show the existence on the northern side of the transform of a major 800-km-long aseismic valley oriented 10° to 15° from the active valley; it disappears about 150 km from the western MAR segment. The aseismic valley marks probably the former location of the Romanche transform ("PaleoRomanche") that was active up to roughly 8-10 Ma, when the transform boundary migrated to its present position. A temporary microplate developed during the migration and reorientation of the transform. This microplate changed its sense of motion as it was transferred from the South American to the African plate. A prominent transverse ridge extends for several hundred kilometers parallel to the transform on its northern side, reaching its shallowest part (shallower by over 4 km than the predicted thermal contraction depth) in a zone opposite the eastern MAR axis/transform intersection (RTI). Flat-top peaks on the summit of the transverse ridge are capped by acoustically transparent, weakly stratified, shallow water platform/lagunal/reef limestones. This limestone unit is a few hundred meters thick and overlies igneous basement. Evaluation of the seismic reflection data as well as study of samples of carbonates, ventifact basaltic pebbles and gabbroic, peridotitic and basaltic rocks recovered at different sites on the transverse ridge, suggest that (1) the summit of the transverse ridge was above sea level at and before about 5 Ma; (2) the transverse ridge subsided since then at an average rate 1 order of magnitude faster than the predicted thermal contraction rate; its summit was flattened by erosion at sea level during subsidence; (3) the transverse ridge is an uplifted sliver of lithosphere and not a volcanic constructional feature; and (4) transtensional and transpressional tectonics have affected the transverse ridge. Hypotheses on the origin of the Romanche transverse ridge include (1) lateral heat conduction across the RTI; (2) shear heating; (3) lithospheric flexure due to thermal stresses in the cooling lithosphere; (4) viscoelastic deformation of the lithosphere; (5) hydration/dehydration of mantle peridotites; and (6) longitudinal flow of melt and igneous activity across the RTI. These processes cannot by themselves explain the transverse ridge, although some of them could contribute to its formation to a small extent. Vertical tectonics due to transpressional and transtensional events related to a nonstraight transform boundary and to regional changes in ridge/transform geometry is probably the primary process that gave rise to the uplift of the transverse ridge and to its recent subsidence. Uplift may have been caused primarily by thrust faulting induced by transpression related to the oblique impact of the lithospheric plate against the former (PaleoRomanche) and the younger transform boundaries, before and during the transition to the present boundary. After migration of the transform boundary to its present position, transpression was replaced by transtension and by subsidence of the transverse ridge. An aseismic axial rift valley impacting against the transform valley about 80 km west of the present RTI suggests eastward ridge jumping that probably followed transform migration. Localized transtension or transpression due to bends in the orientation of the transform may have caused intense although localized vertical movements, such as those that formed an ultradeep (>7800 m) pull-apart basin along the transform valley.

[1]Istituto Geologia Marina, Consiglio Nazionale delle Ricerche, Bologna, Italy and Lamont-Doherty Earth Observatory, Palisades, New York.

[2]Istituto Geologia Marina, Consiglio Nazionale delle Ricerche, Bologna, Italy.

[3]Geology Institute, Russian Academy of Sciences, Moscow.

[4]College of Oceanography, Oregon State University, Corvallis.

Paper number 94JB01178.
0148-0227/94/94JB-01178$05.00

Introduction

The Mid-Atlantic Ridge (MAR) is offset in the equatorial Atlantic by a set of closely spaced long transforms (Plate 1). Very large topographic anomalies are found in this region, particularly as transform-parallel ridges (transverse ridges) that can rise several kilometers above predicted thermal contraction crustal levels [*Van Andel et al.*, 1971; *Bonatti*, 1978]. In the equatorial Atlantic these transverse ridges, together with the deep valleys typical of long offset slow-slip transform zones, cause some of the roughest topography found anywhere in the ocean basins.

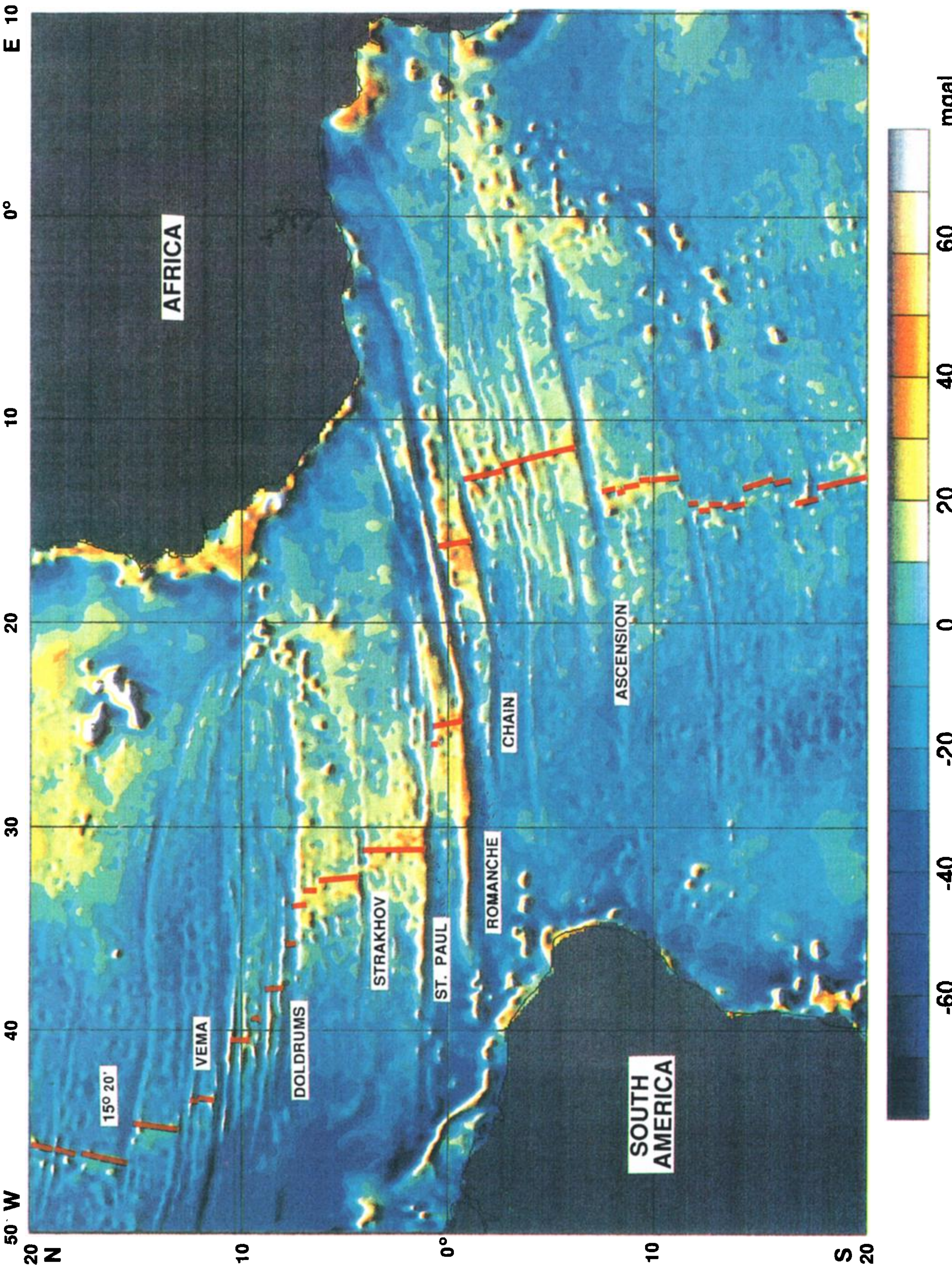
AFRICA
SOUTH AMERICA
15° 20'
VEMA
DOLDRUMS
STRAKHOV
ST. PAUL
ROMANCHE
CHAIN
ASCENSION
mgal
60
40
20
0
-20
-40
-60
E 10
0°
10
20
30
40
50 W
20 N
10
0°
10
S 20

In this paper we report some results of a field study of the eastern end of the Romanche transform near the equator. The field work included multichannel high-resolution seismic reflection, multibeam, and magnetometric surveys as well as rock and sediment sampling. It was carried out from November 1991 to January 1992 with the vessel *Akademic Nikolai Strakhov* of the Geology Institute of the Russian Academy of Science. This work is part of the Russian-Italian Mid-Atlantic Ridge Project (PRIMAR).

One of the objectives of this work is to understand processes related to the reorientation and migration of major transform boundaries in this region and to the formation of the prominent topographic anomalies found in the equatorial Atlantic.

Background: Romanche Transform

The Romanche transform offsets the axis of the MAR by about 950 km; it is thus the longest active transform of the entire mid-ocean ridge system [*Heezen et al.*, 1964]. Seasat/Geosat gravity imagery [*Haxby*, 1987] shows that the Romanche fracture zone can be traced across the equatorial Atlantic from an offset of the Gulf of Guinea continental shelf to an E-W branch of the North Brazilian Ridge on the American side (Plate 1). Thus the Romanche probably originated as a continent/continent transform at the time of initial rifting of the proto-Atlantic.

The Romanche is characterized by a deep, roughly E-W valley flanked on both sides by two prominent ridges and by a system of secondary parallel troughs and ridges [*Heezen et al.*, 1964; *Gorini*, 1977; *Chermak*, 1979]. The deepest part of the valley, reaching about 7.8 km below sea level, is located between 18° and 19°W. The shallowest depths are reached in the narrow transverse ridge flanking the northern side of the transform, east of about 18°W. This constitutes a major topographic anomaly that rises up to 4 km above the level predicted by the thermal contraction depth-(age)$^{1/2}$ law, if we assume a constant ridge/transform geometry and an average spreading rate of 1.75 cm/yr (half rate) both north and south of the transform for the last 50 m.y. This spreading rate is derived from plate kinematic reconstructions of *Cande et al.* [1988]. With these assumptions the crust affected by the topographic anomaly ranges in age roughly from $\simeq$35 to $\simeq$55 Ma. Previous work has indicated that the summit of the transverse ridge was above sea level up to about 5 Ma and subsided since then at a rate 1 order of magnitude faster than the plate thermal subsidence rate [*Bonatti et al.*, 1979a, b; *Bonatti and Chermak*, 1981].

Methods

The ship's position was determined with a Global Positioning System (GPS) NAVSTAR satellite navigation system, with an accuracy of ±25 m. Morphobathymetry was obtained with a Hollming Echos 625 multibeam system, consisting of 15 (12.5 kHz) beams covering a swath of seafloor roughly 2/3 water depth in width. Rock and sediment sampling were carried out by conventional dredging and coring methods. Seismic reflection data were obtained using a Sodera GI-GUN as sound source. It operated in harmonic mode configuration, with the capacity of 105 cubic inches for the generator as well as for the injector, at the pressure of 2000 psi. The receiving streamer employed 24 channels (each with 20 hydrophones) spaced 25 m apart. Seismic source and nearest channel were spaced 150 m apart. Shot interval was 50 m, allowing sixfold coverage. Digital acquisition was carried out with a Geometrics 2420, with a sampling rate of 1 ms, a record length of 11 s, and an antialias filter of 180 Hz. Seismic data have been processed at the Institute of Marine Geology of the Consiglio Nazionale delle Ricerche (CNR) of Bologna using an industrial standard package (DISCO) made by CogniSeis.

Results

A synthesis of available bathymetric data from the Romanche region, including our own and those of *Monti and Mercier* [1991], *Honnorez et al.* [1991], and *Searle et al.* [1994], has been processed to produce a shaded relief image of the region, shown in Figure 1. Of the many features displayed by this map we note that (1) the transverse ridge rises prominently on the northern edge of the transform zone opposite to the eastern ridge-transform intersection (RTI); (2) the eastern RTI is not well defined morphologically, contrary to the western RTI (where, however, data coverage is not as good); (3) the active transform valley, defined on the basis of earthquake epicenters, is not straight, but its orientation has a few discrete "bends"; and (4) a more or less continuous aseismic valley extends north of and is subparallel to the main transform valley. We present some additional data for each of these features.

Romanche Transverse Ridge

The shallowest (<2000 m below sea level) stretch of the transverse ridge is located roughly opposite the eastern RTI (Plate 2 and Figures 2 and 3). As noted by *Honnorez et al.* [1991] and *Mamaloukas-Frangoulis* [1992] and as clearly shown by the three-dimensional (3-D) imagery of Figure 3, the transverse ridge is asymmetric in N-S sections, its north facing slope being less steep than the south facing one. Moreover, the south facing slope is interrupted by a suspended valley striking about 10°-15° from the strike of the present active transform valley. The suspended valley deepens toward the east and merges with the presently active transform valley at about the longitude of the eastern RTI. The suspended valley constitutes the eastern termination of an aseismic valley running for several hundred kilometers on the northern side of the seismic transform valley (Figure 1 and Plate 2). The shallowest (<2000 m) portion of the transverse ridge displays a number of peaks elongated roughly E-W. We identify them from west to east as peaks A, B, C and D (Figure 2). Samples were obtained from different sites on the transverse ridge during this and previous expeditions. A roughly E-W seismic reflection line was carried out along the crest of the transverse ridge (line ROM-2, Figure 4) and three lines were run roughly normal to it (ROM-1, ROM-3 and ROM-5, Figure 4). We describe these peaks based on the seismic reflection data and the samples obtained from them.

Plate 1. Seasat and Geosat gravity imagery of the equatorial Atlantic, compiled by W.F. Haxby. The trend of the Mid-Atlantic Ridge axis and the names of the major fracture zones have been superimposed .

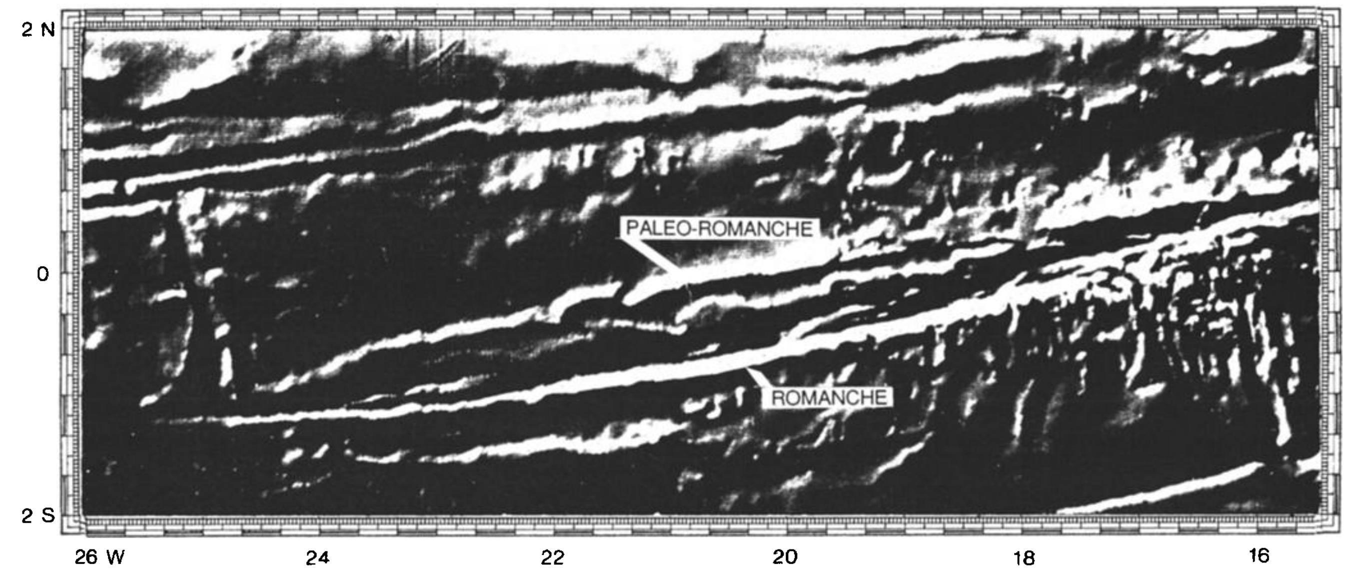

Figure 1. Shaded relief map of the Romanche transform region, derived by bathymetric data from *Heezen et al.* [1964], *Gorini* [1977], *Chermak* [1979], *Honnorez et al.* [1991], *Monti and Mercier* [1991], *Searle et al.* [1994], and our own data.The shaded relief map was obtained assuming illumination from NW 45° over the horizon. Horizontal resolution is 1 km, no vertical exaggeration. Mercator projection at 0°.

Peak A

This is the shallowest peak, reaching 930 m below sea level. Samples obtained from and near its summit (Figure 4) consist of shallow water reef/lagunal limestones. Paleofacies analyses suggest that these limestones formed in shallow (-50 m) carbonate banks and lagoons and subsequently underwent subaerial diagenesis, indicating that the top of this structure emerged as an island sometime in the past [*Bonatti et al.*, 1979b; *Bonatti and Chermak*, 1981]. This interpretation was supported recently by the recovery from the western slope of peak A of basalt pebbles, partly cemented by carbonates, showing ventifact morphology that implies subaerial exposure [*Honnorez et al.*, 1991].

Profile ROM-2 (Figure 5) shows that peak A consists of an upper semitransparent unit, about 300 ms thick, separated from an opaque substratum by a strong, more or less horizontal reflector. Based on samples obtained from peak A, we interpret this sequence as indicating a platform of semiconsolidated carbonate deposits capping igneous basement. Assuming a sound velocity of 2 km/s for the upper unit, its thickness reaches about 300 m. The western part of the profile on peak A shows a shallow basin about 5 km wide with layered sediments prograding westward from the platform into the basin. The basin is bound on the west by a nontransparent, $\simeq$70 m high structure (Figure 5). We interpret this sequence as a former shallow lagoon edged by semiconsolidated carbonate reefs. Thus both seismic reflection data and dredged samples are consistent with the idea that peak A is a sunken fossil atoll, resting, however, not on a volcanic constructional substratum but on an uplifted sliver of oceanic lithosphere. The nearly horizontal top of the igneous basement, represented by the prominent horizontal reflector, suggests wave truncation during subsidence.

Age determinations based on planktonic foraminifera and on *Stylophora sp.* corals date the shallow water carbonates sampled from peak A at the Miocene-Pliocene boundary, about 5±1 Ma. Assuming the summit of the peak was at sea level at that time and that sea level at the end of the Miocene was within 100 m of present-day sea level [*Shackleton and Kennett*, 1975; *Vail and Hardenbol*, 1979; *Haq et al.*, 1988], an average subsidence rate of 0.2 mm/yr can be estimated. This rate is 1 order of magnitude faster than the thermal subsidence estimated for 50 Ma crust [*Bonatti et al.*, 1979b, *Bonatti and Chermak*, 1981].

Peak B

The stretch of ROM-2 reflection profile over peak B shows a feature capped by semitransparent 250-ms-thick material separated from the opaque substratum by a strong horizontal reflector (Figure 6). We interpret this profile as indicating a semiconsolidated carbonate cap about 250 m thick resting on igneous basement. Smooth, rounded basaltic pebbles, as well as pebbles with characteristic "ventifact" morphology, both covered by a thin (<1 mm) patina of Fe-Mn oxides, were recovered by us near the summit of peak B (station S13-48, Figure 4). They suggest reworking in a beach environment and subaerial exposure, implying that also the summit of peak B reached above sea level. The horizontal reflector marks the eroded top of the oceanic crust.

Peak C

The reflection profile shows a semitransparent, weakly stratified platform about 300 ms thick, separated from the opaque substratum by a strong, nearly horizontal reflector (Figure 7). Shallow water platform-reef-lagunal limestones similar to those of peak A were recovered from the upper slopes of peak C (Figure 4, station GS7309-59), implying that also peak C reached close to sea level sometime in the past, although no age diagnostic fossils were found. As in peaks A and B, the horizontal reflector is interpreted as the top of the oceanic crust flattened by erosion at sea level during subsidence.

We note that the depth below sea level of the horizontal reflector (i.e., of the erosional surface of the igneous basement) is similar for peaks A, B, and C, i.e., 1355 m ±50, implying that a ~100-km-long stretch of transverse ridge subsided as a single block.

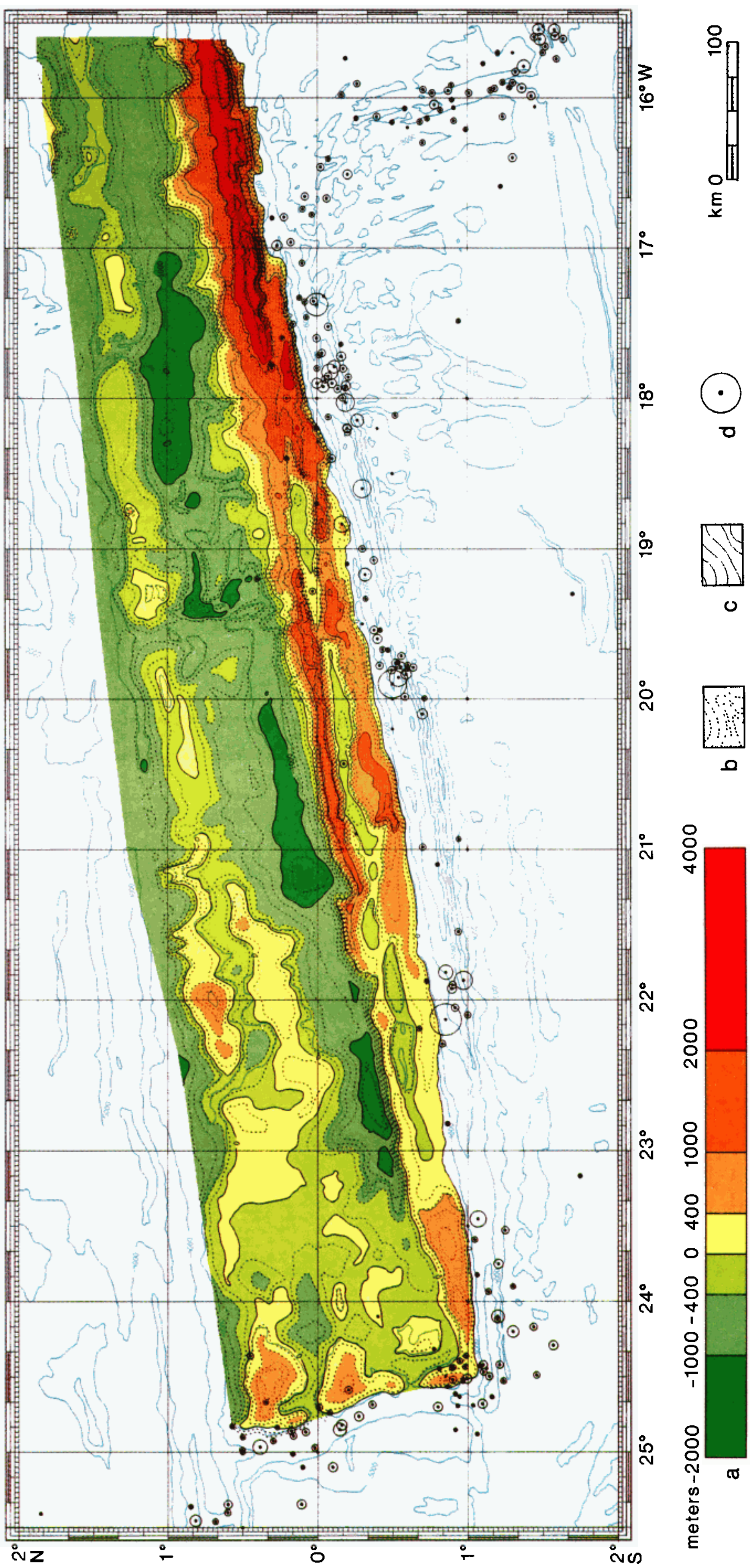

Plate 2. Topographic anomaly contour map relative to the theoretical thermal contraction level of the crust [*Parsons and Sclater*, 1977] for the northern side of the Romanche transform. a, range of topographic anomalies (in meters) plus or minus the theoretical level; b, isoanomaly curves (in meters), interval 200 m; c, bathymetric curves (in meters), interval 1000 m; d, earthquake epicenters, 1960-1990.

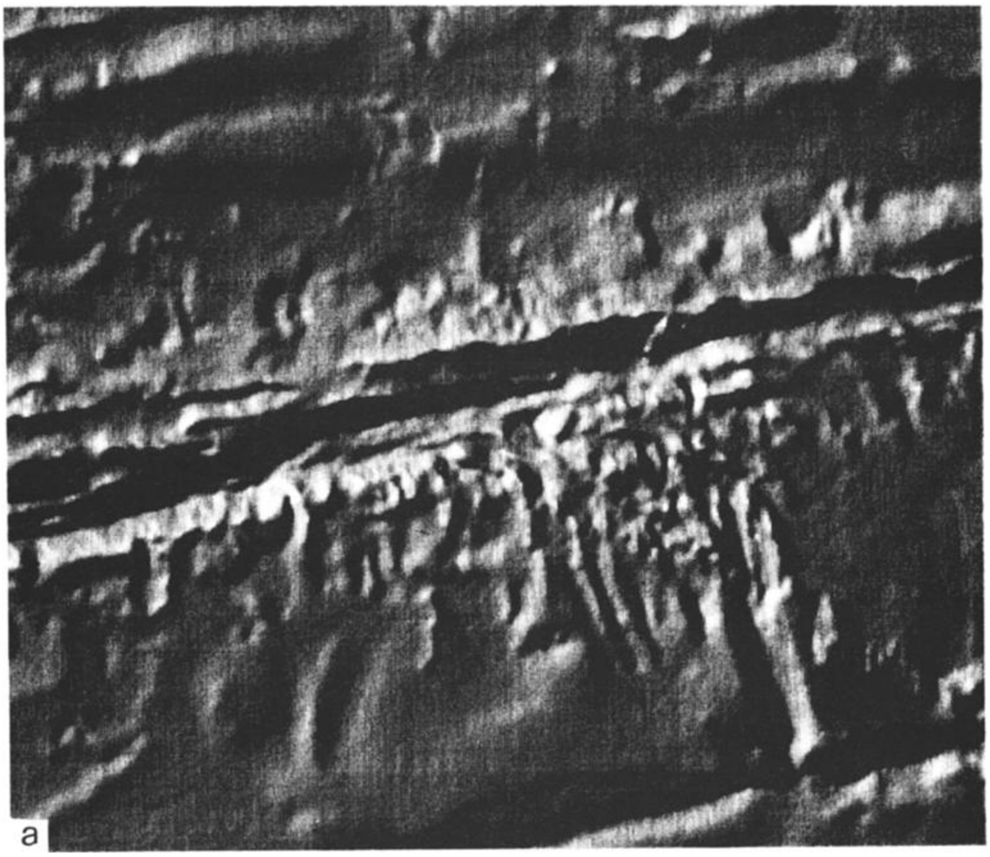
a

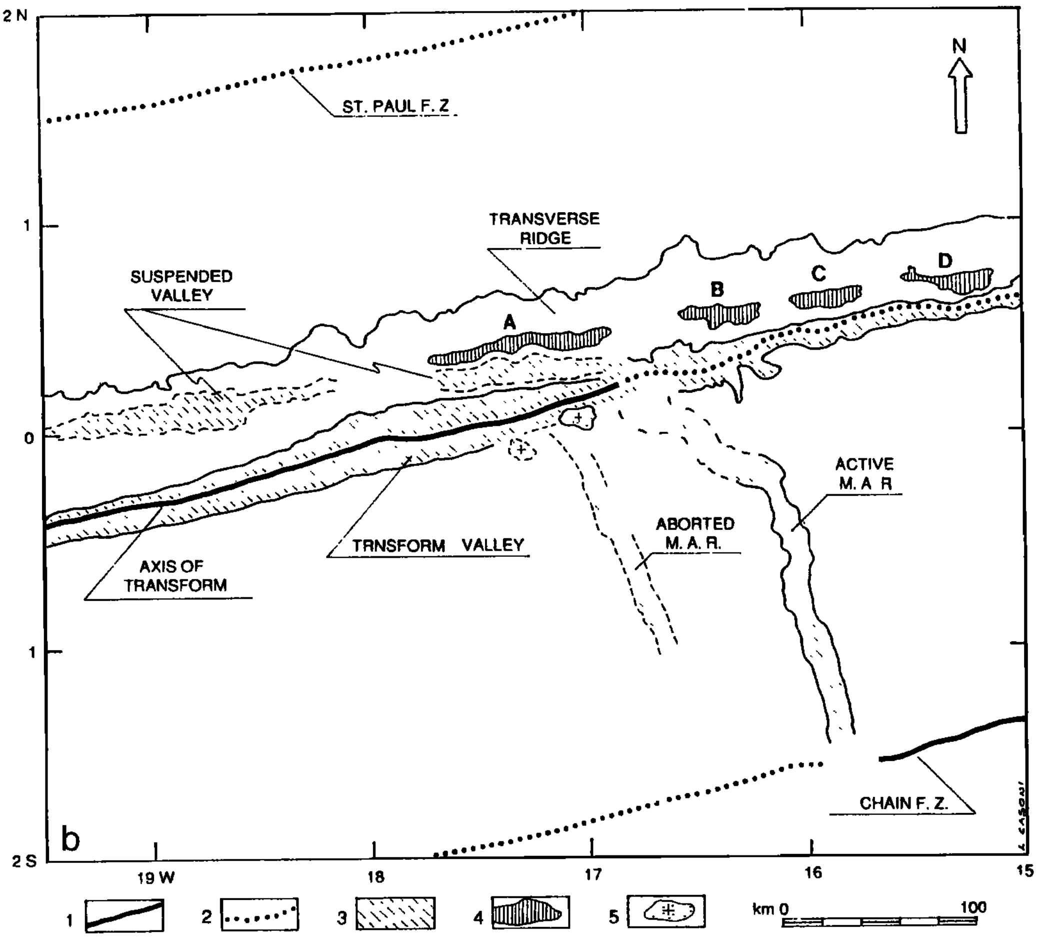
2 N
1
0
1
2 S
19 W
18
17
16
15
N
ST. PAUL F. Z
TRANSVERSE
RIDGE
SUSPENDED
VALLEY
A
B
C
D
ACTIVE
M. A R
ABORTED
M. A. R.
TRNSFORM VALLEY
AXIS OF
TRANSFORM
CHAIN F. Z.
b
1
2
3
4
5
km 0
100

Peak D

This peak has a very different character from peaks A, B, and C (Figure 8). Peak D does not show evidence of a carbonate platform built on a horizontal erosional surface. Contrary to the profiles obtained from peaks A, B and C, where the substratum below the limestone cap (presumably the oceanic igneous crust) does not give clear coherent reflections, the seismic data for peak D show continuous "real" reflectors down to about 8 s. Although we do not have any direct information on sound velocities, we exclude that our sound source could achieve such deep penetration if peak D were a sliver of igneous oceanic crust. This and the character of the reflections suggest that the profile images a thick pile of sedimentary rocks, perhaps with intercalation and lenses of volcanic rocks. If we assume a sound velocity of not less than 2 km/s, the thickness of the sediment pile is at least 4 km. This is a minimum thickness because it is probable that the thick sequence consists at least in part of consolidated or semi-consolidated units, with acoustic velocities >2 km/s, as also indicated by samples recovered from peak D. The character of the reflections calls for units affected by folds and overthrust, in a tectonic style suggestive of a compressional regime. Contact between the portion of the transverse ridge made of uplifted oceanic crust, and that to the east made of a thick sedimentary pile, is marked on profile ROM-2 by a reflection with an apparent dip toward the east that can be followed down to 8 s depth (Figure 8).

Sedimentary rocks dredged from peak D (station GS 7309-63, Figure 4) consist of consolidated laminated siltites, micritic limestones, and radiolarian micrites and cherts, to be described elsewhere.

Eastern Ridge/Transform Intersection

Our morphobathymetric compilation of the Romanche eastern RTI region (Plate 2 and Figures 2 and 3 and unpublished data (1993)) is based on a dense multibeam and conventional coverage that includes our own multibeam surveys. A well-formed MAR axial rift valley is not present in the southern side of the fracture zone valley and is replaced by an area with diffuse seismicity and with en echelon short and poorly developed axial ridge segments. An unambiguous active nodal basin was not identified. About 80 km to the west of this poorly developed RTI a well-formed aseismic valley meets the transform valley in what is probably a fossil RTI.

Inactive Transform Valley

The shaded relief morphobathymetric imagery of the Romanche region (Figure 1) shows that an aseismic valley extends for about 800 km from the vicinity of the eastern RTI to about 150 km from the western MAR segment. The eastern part of the inactive valley is suspended on the southern slope of the transverse ridge and merges with the active transform valley in the general area of the RTI (Figures 2 and 3).

Seismic reflection profile ROM-3 (Figure 4) extends approximately N-S from the crest and the southern slope of the transverse ridge across the suspended valley down to the bottom of the presently active transform valley (Figure 9). The suspended valley contains a considerable thickness ($\simeq$500 ms two-way-time (TWT)) of weakly stratified sediment; assuming a sound velocity of 1.8 km/s, this would amount to a thickness of $\simeq$450 m. The basement appears to be affected by extensional tectonics, with sets of low-angle listric faults and smaller antithetic faults dipping in the opposite direction. Rotation of blocks may have occurred on south dipping planes. The thick sediment pile overlying basement does not appear to be affected by extensional tectonics, although the geometry of the strata is not regular, and angular discordances are common.

Transform Migration and Reorientation

Reconstruction of past MAR/transform geometries is a difficult task in the equatorial Atlantic due particularly to the poor development of magnetic anomalies in the equatorial belt. This notwithstanding, the following data strongly suggest a non-steady state MAR axis/transform geometry in the equatorial area.

1. The eastern Romanche RTI is poorly defined morphologically and petrologically. An axial rift valley appears to be well developed in the southern part of the MAR segment between the Romanche and the Chain transforms. However, it fades out about 80 km from the Romanche transform valley (Figure 2), where it is replaced by a set of en enchelon, poorly developed rift segments that disappear completely about 30 km from the edge of the valley. Our dense sampling program indicates that mantle peridotites outcrop throughout this area, where a basaltic crust is absent. It appears therefore that a diffuse rifted zone rather than a normal rifted axis of spreading meets the Romanche transform at its eastern RTI. This diffuse rifted zone is defined mostly by the location of earthquake epicenters.

2. The presence about 80 km west of the presently active RTI area of a well-formed aseismic rift valley, filled with an about 200-m-thick sediment pile, coupled with the poorly developed present RTI, suggests a process of ridge jumping. Abrupt appearance in our seismic profiles of a thick (>200 m) sediment cover about 50 km to the east and west of the presently active diffuse ridge axis suggests that the diffusely active MAR segment presently impinging against the eastern end of the Romanche transform was emplaced into older crust <5 Ma, if we assume a 1.75 cm/yr spreading rate [*Cande et al.*, 1988].

3. The major aseismic E-W valley, identified on the northern side of the presently active Romanche transform valley (Figure 1), is interpreted by us as the trace of a former transform boundary, which we call the PaleoRomanche transform. The observation that the inactive valley contains several hundred meters of sediments, in contrast to the active transform valley where sediment cover is scant (Figure 9), implies that the presently active transform valley is a relatively young feature and the inactive valley has existed for a long time. Given that

Figure 2. (opposite) (a) Shaded relief map (a) and (b) simplified morphology of a stretch of the transverse ridge, roughly opposite to eastern RTI, showing the position of the shallowest peaks on the crest. They are identified from west to east as peaks A,B,C and D. 1, trace of the axis of the active trasform valley; 2, axis of the inactive fracture zone valley; 3, bottom of valleys; 4, summit (<2000 m) of peaks on the crest of transverse ridge; 5, inferred "fossil" inner corner highs. Shaded relief map was obtained assuming illumination from NW 45° over the horizon. Horizontal resolution is 0.5 km, vertical exaggeration 4X. Mercator projection at 0°.

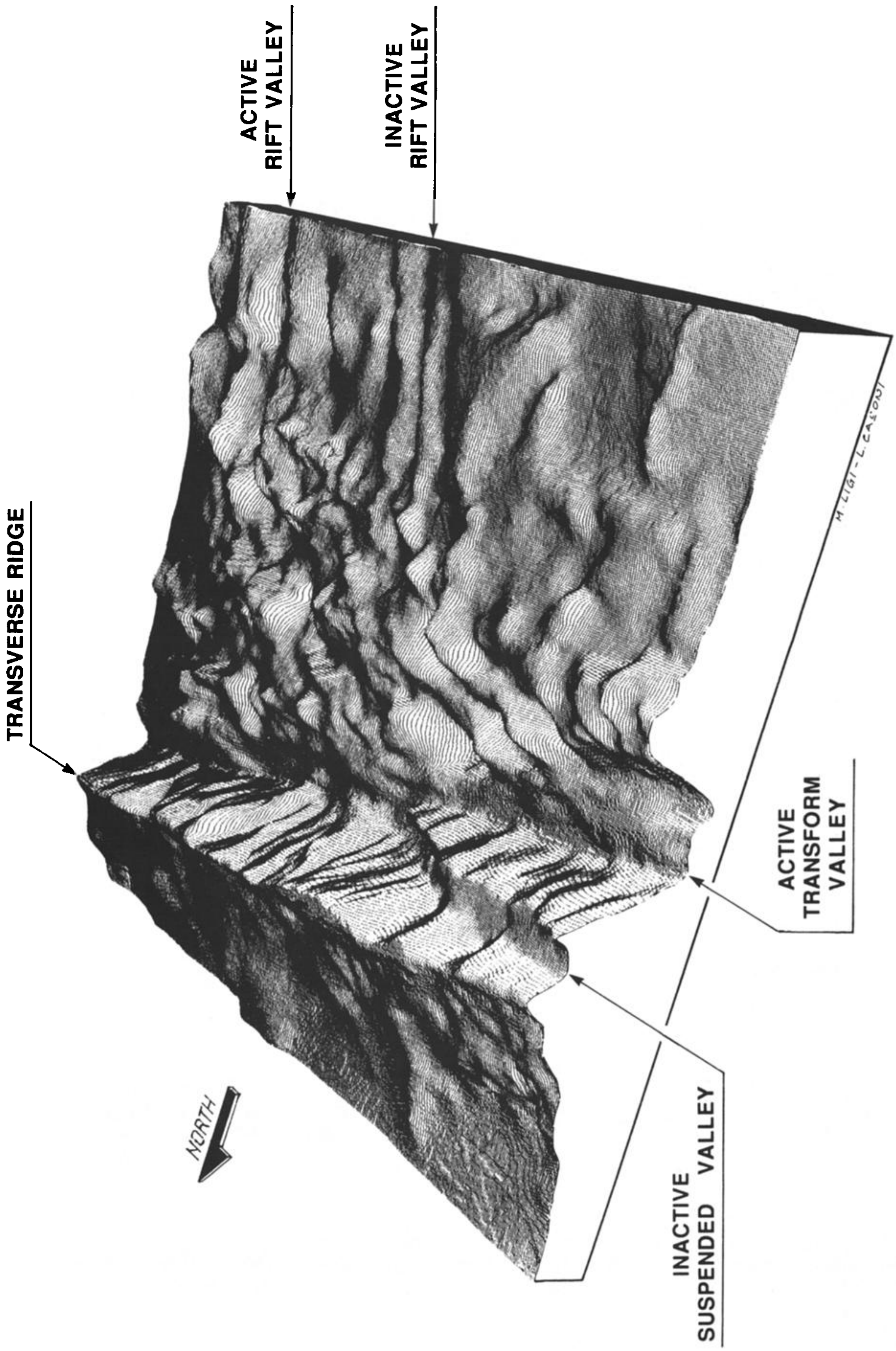

Figure 3. Three-dimensional morphobathymetric image of the eastern part of the Romanche transform. Source of data is as in Figure 1. Vertical exaggeration is about 12.5 times.

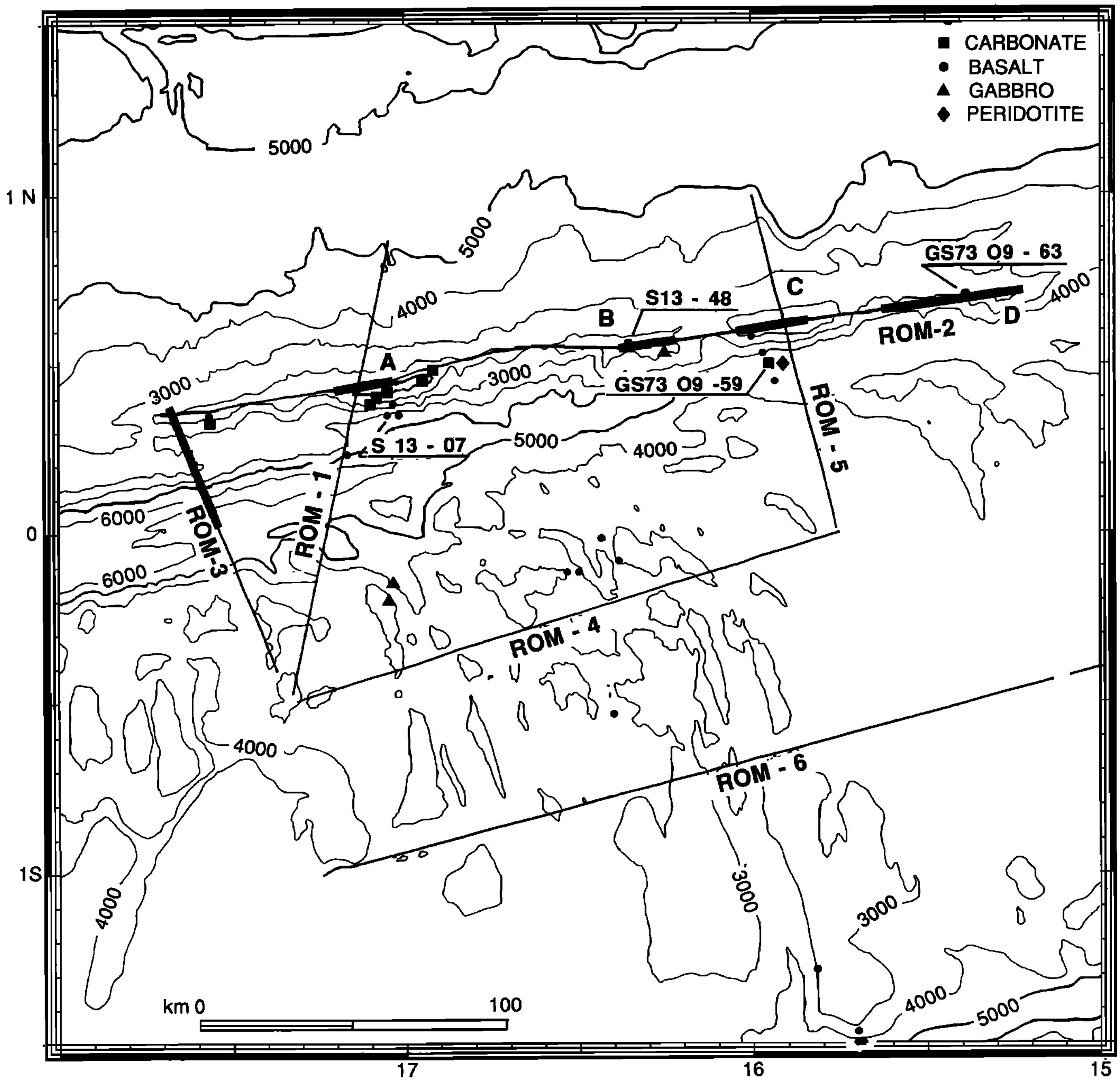

Figure 4. Tracks of seismic reflection profiles carried out during Cruise S-13. The portions of the profiles shown in Figures 5, 6, 7, 8, and 9 are marked with a thicker line. Sites where rock samples were recovered are also indicated with different symbols for different rock types.

the aseismic valley dies out roughly 150 km from the western MAR segment, and assuming a 1.7 cm/yr spreading rate, we estimate that the PaleoRomanche ceased to be active about 8-10 Ma, after which the transform boundary migrated to its present position.

The old and the new transforms are not parallel, but their orientation differs by up to about 15°, particularly in the eastern part. We have digitized at 10 arc min intervals the position of the axis of the PaleoRomanche valley and estimated the small circle with the best fit to it. We then calculated the pole of rotation pertaining to this small circle, according to *Searle*'s [1981] method. The "best fit pole" relative to the PaleoRomanche is at 75°.20N and 62°.77W. *Searle*'s [1981] method does not allow a good estimate of the distance of the pole from the transform primarily due to the short length of the fossil PaleoRomanche. However, the azimuth (±1°) is well constrained. Figure 10 shows the "stage pole" position (Africa relative to South America) calculated by *Cande et al.* [1988], the fossil transform's pole with its 95% confidence level ellipse and the poles calculated by *Minster and Jordan* [1978] and *Searle et al.* [1994]. We note that *Cande et al.*'s [1988] Africa/South America pole for magnetic anomalies 6-5 (19.3 to 8.9 Ma) falls within the range of possible pole position estimated from the PaleoRomanche fossil transform. This supports the idea that the inactive valley represents a formerly active trace of the Romanche transform.

Migration and reorientation of a long-offset, slow slip

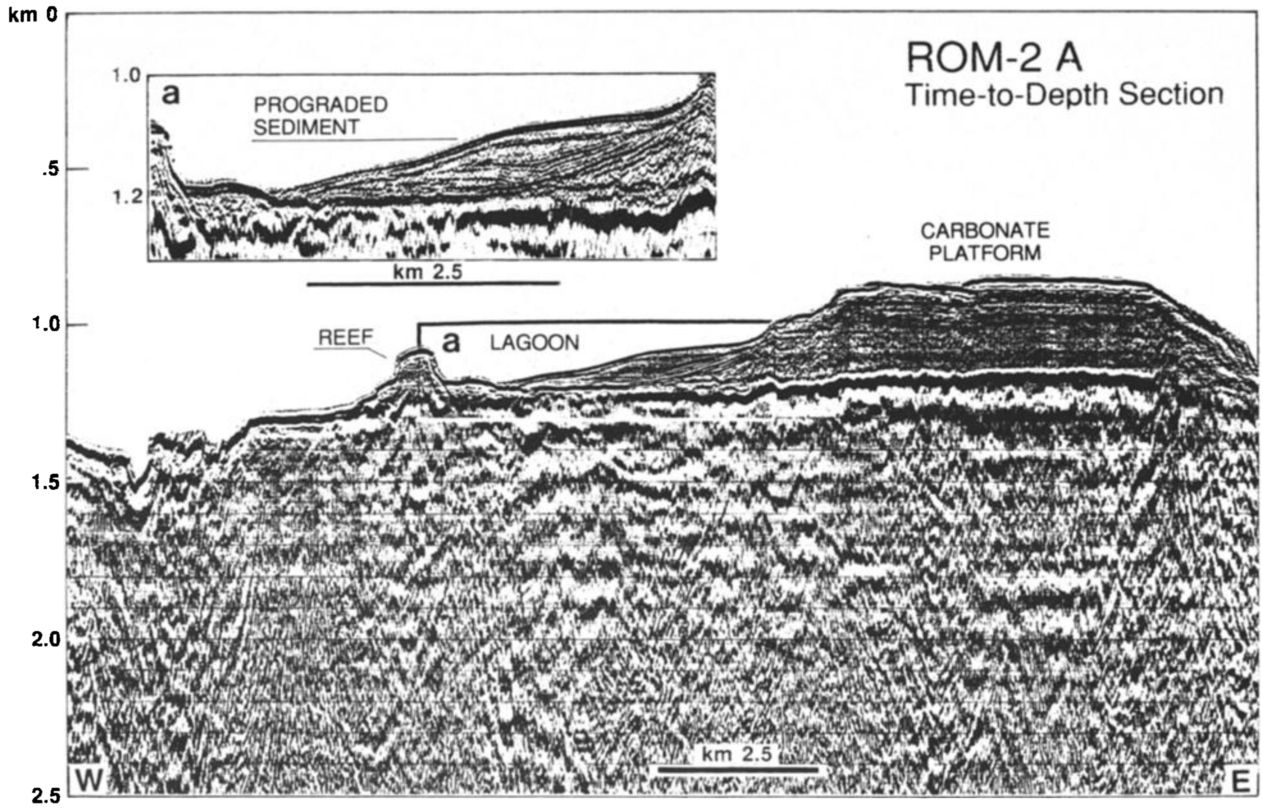

Figure 5. Portion of seismic reflection profile ROM-2 over peak A (time-to-depth converted section). Location of this profile is shown in Figure 4.

transform such as Romanche, involving thick lithosphere as old as 50 Ma, surely must imply a major geotectonic upheaval. It probably involves ridge propagation on one side, and ridge-tip truncation or decapitation on the other side. A tentative sequence of events is shown in Figure 11. A noninstantaneous transition from the old to the new geometry implies the creation of a temporary Romanche microplate that includes the sliver of lithosphere between the old and the new transform. This sliver of lithosphere would be transferred from the South American to the African plate during the transition and would reverse its sense of motion in a process that has been called "oscillatory spreading" [*Bonatti and Crane*, 1982].

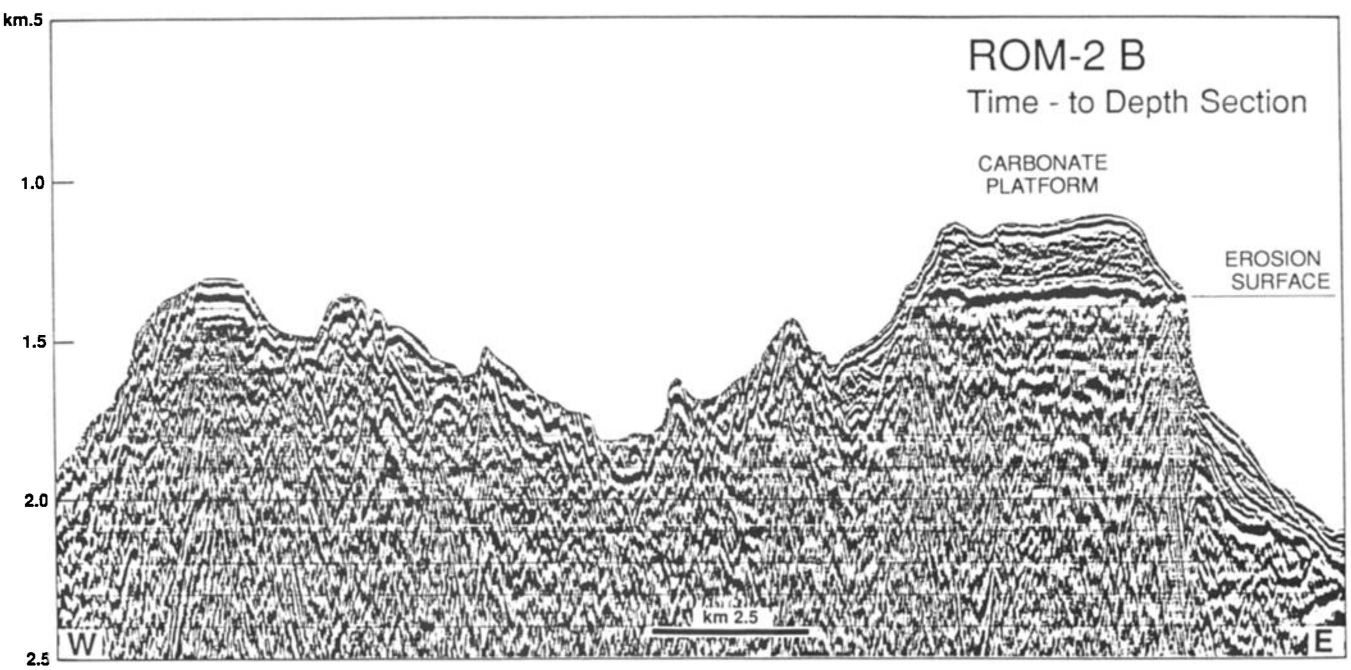

Figure 6. Portion of seismic reflection profile ROM-2 over peak B (time-to-depth converted section). Location of this profile is shown in Figure 4.

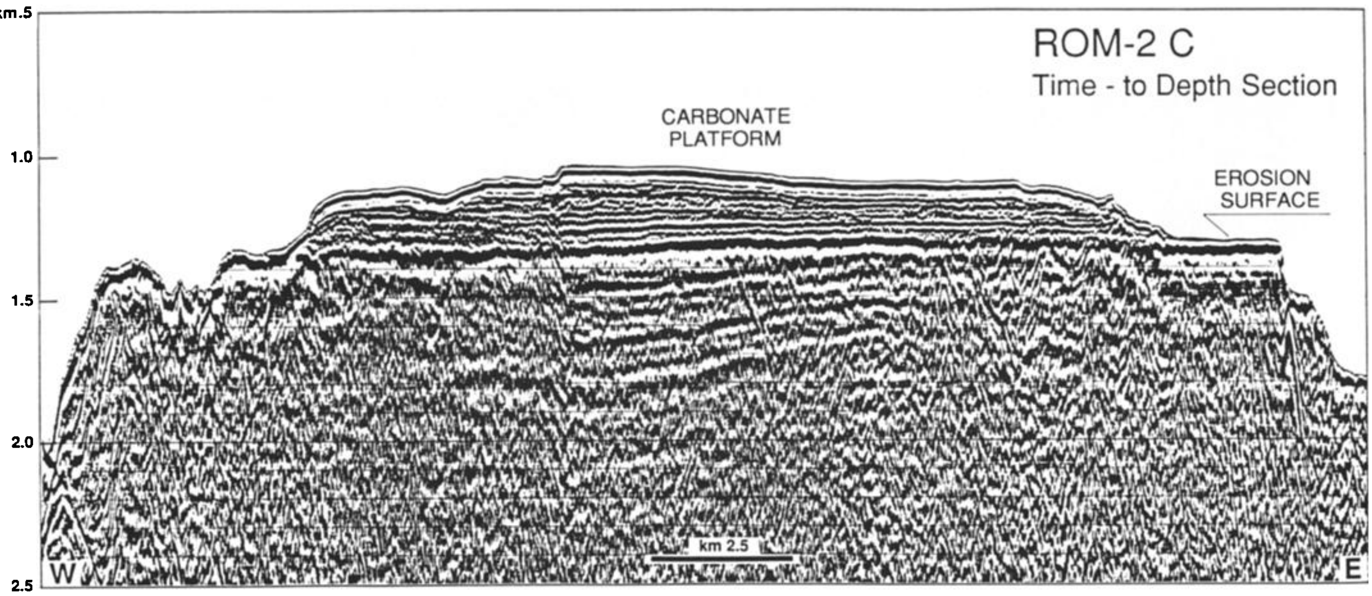

Figure 7. Portion of seismic reflection profile ROM-2 over peak C (time-to-depth converted section). Location of this profile is shown in Figure 4.

Origin of Romanche Transverse Ridge

We have estimated the shape and extent of the topographic anomaly on the northern side of the Romanche transform relative to the predicted thermal contraction level using our compilation of available bathymetric data (Plate 2). An isopach chart was compiled on a 1 km by 1 km grid, where sediment thickness was estimated from single-channel and multichannel seismic reflection profiles of *Gorini* [1977], *Chermak* [1979], and our own expedition, assuming a sound velocity of 2 km/s. Crustal ages were calculated on a 1 km by 1 km grid based on distance from the MAR axial segment

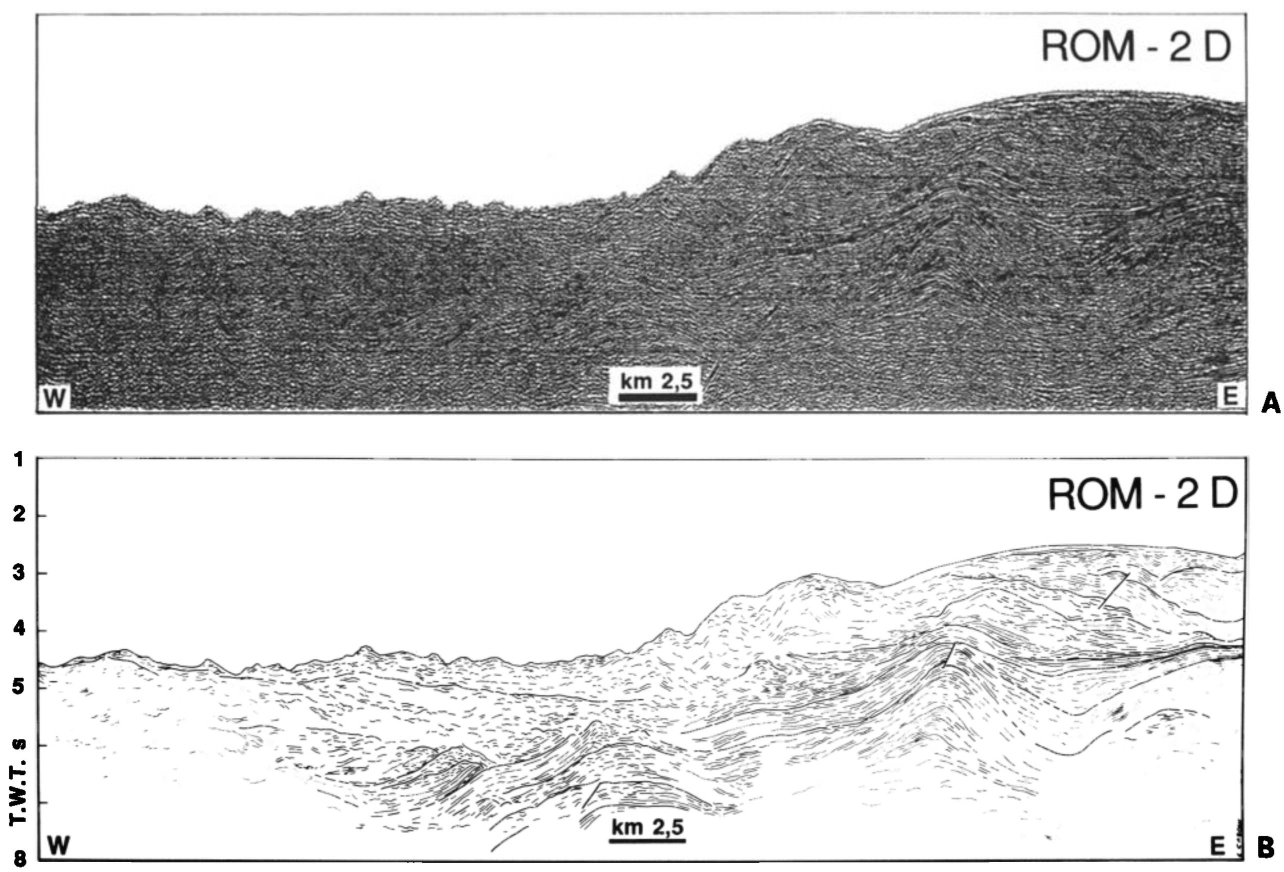

Figure 8. Portion of seismic reflection profile ROM-2 over peak D (time-to-depth converted section). Location of this profile is shown in Figure 4. (a) Migrated time section and (b) interpreted line drawing.

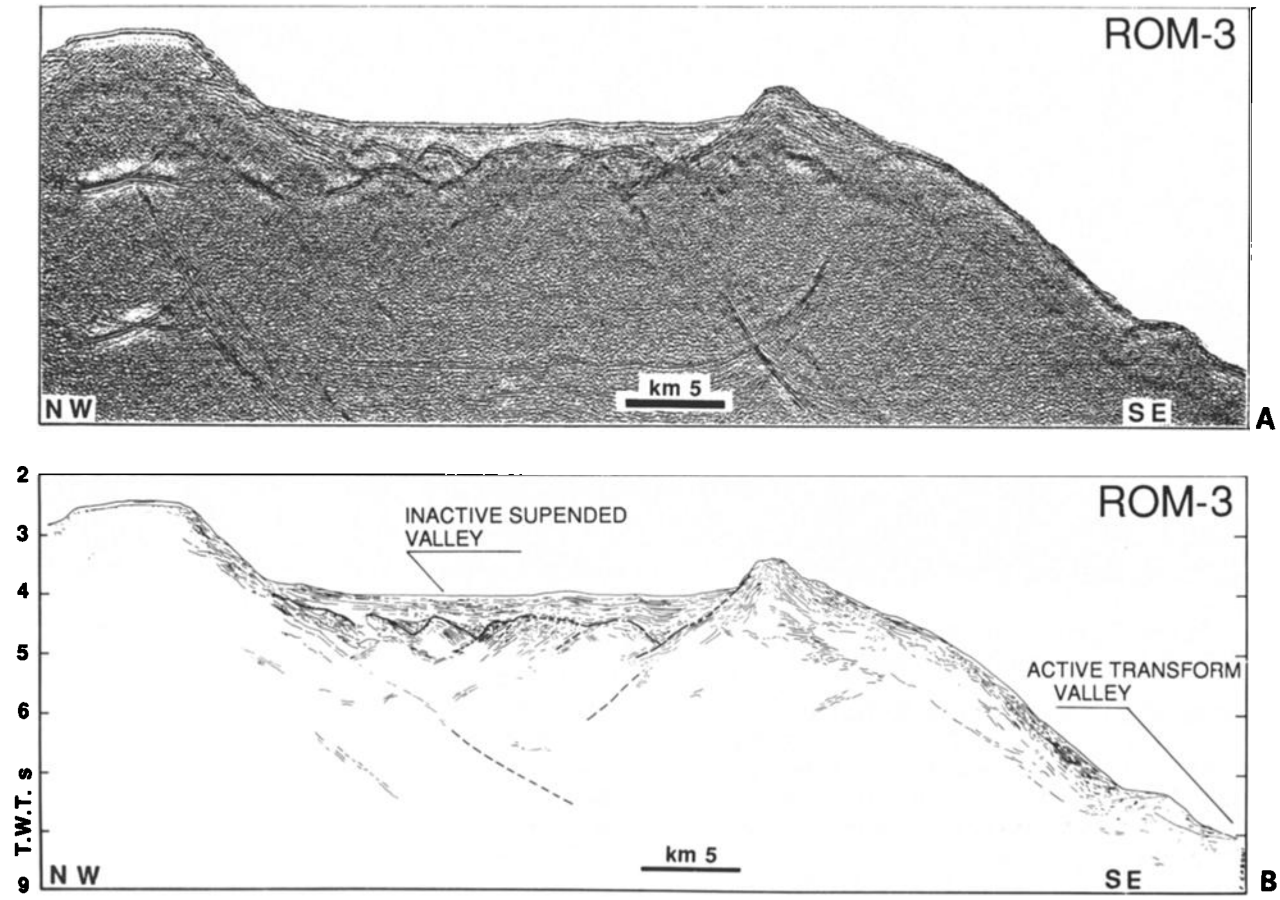

Figure 9. Portion of seismic reflection profile profile ROM-3 showing the summit and the southern slope of the transverse ridge, including a section of the suspended valley. (a) Migrated time section and (b) interpreted line drawing. Location of this profile is shown in Figure 4.

between Romanche fracture zones (FZ) and St. Paul FZ and on spreading rates calculated by *Cande et al.* [1988].

We applied a correction to account for subsidence related to sediment load. This correction was done assuming Airy isostatic compensation and using the relation [*Steckler and Watts*, 1981]

$$d_c = d_w + F\ [(r_m - r_s)/(r_m - r_w)]\ h$$

where

d_c corrected depth, in meters;
d_w water depth, in meters;
r_m density of the mantle, equal to 3.330 kg/m^3;
r_s density of sediments, equal to 1700 kg/m^3;
r_w density of water, equal to 1000 kg/m^3;
h sediment thickness, in meters;
F function of response of the basement (it varies between 0 (no compensation) and 1 (Airy isostatic compensation) depending on the degree of isostatic compensation by load).

The theoretical depth d(t) of the oceanic basement has been obtained from *Parsons and Sclater's* [1977] relationship $d(t) = 2500 + 350\ t^{1/2}$. The topographic anomaly shown in Plate 2 is the difference between d_c and d(t). It represents the extent to which the topography differs from the theoretical thermal contraction level of the crust. The anomaly reaches over 2 km in a stretch of seafloor extending from slightly east of 18°W to well east of 15°30'W for a length of over 200 km, that is, from roughly 100 km west of the MAR-Romanche eastern intersection to over 100 km east of the intersection, outside the transform zone proper. The >3 km anomalies correspond essentially to peaks A, B, C, and D described in the previous section. The strongest anomaly is peak A; it reaches close to 4 km.

We will now consider a number of factors that may have contributed to the formation of the Romanche topographic anomaly. These factors include thermal rejuvenation of old lithosphere near the RTI; frictional shear heating along the transform; lithospheric flexure due to thermal stresses; nonlinear viscoelastic deformation of the lithosphere; hydration/dehydration reaction of upper mantle rocks near the transform; igneous activity; and transform-related transpression/transtension.

Thermal Rejuvenation of Old Lithosphere Near the RTI

Several authors have discussed three-dimensional models of the thermal structure of transforms and the topographic effect of horizontal conductive heat transfer from the hot young lithosphere to the old plate across the transform [*Langseth and Hobart*, 1976; *Louden and Forsyth*, 1976; *Forsyth and Wilson*, 1984; *Morgan and Forsyth*, 1988; *Chen*, 1988]. According to a model developed by *Chen* [1988] the thermally induced

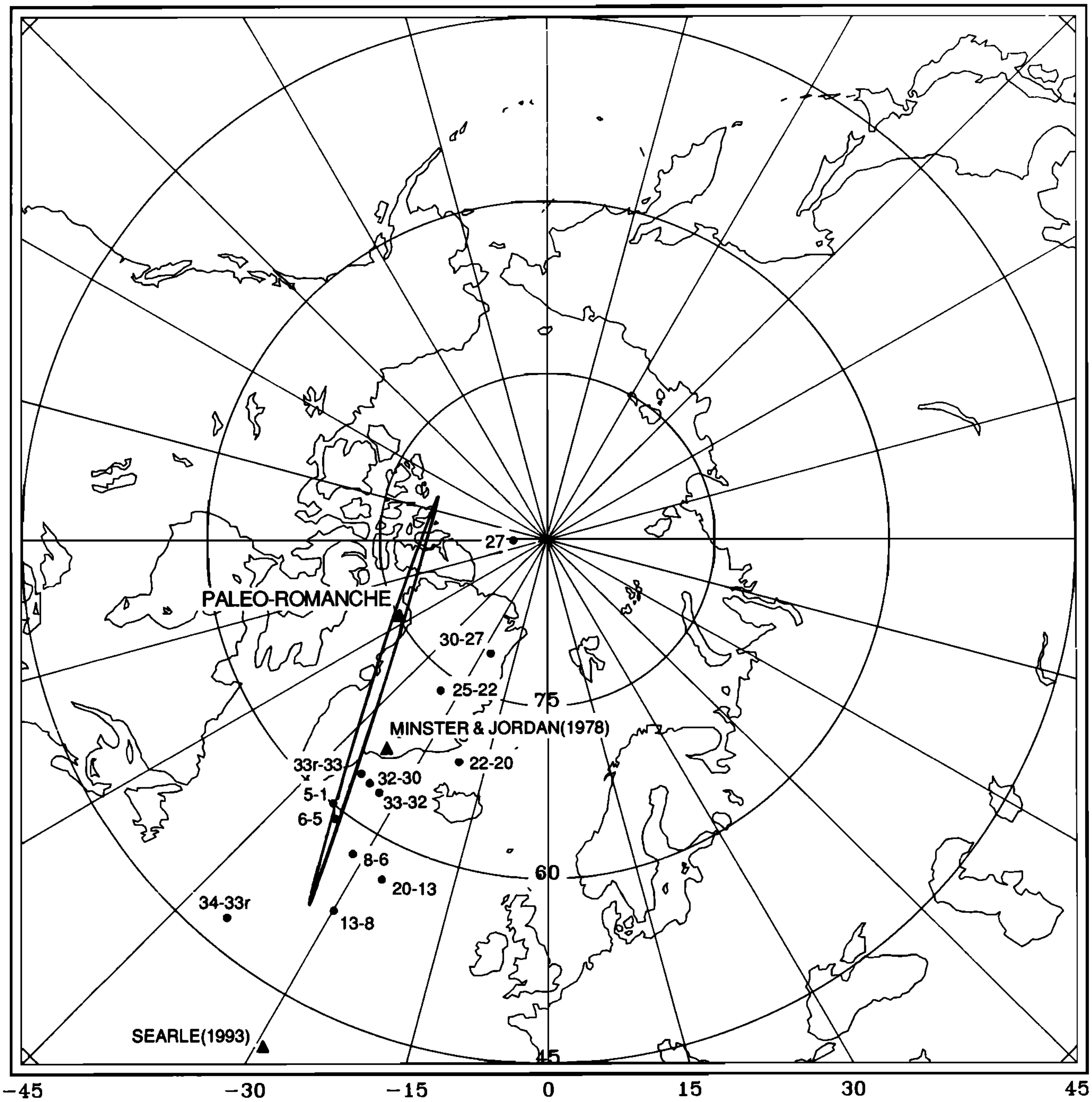

Figure 10. Map showing the "stage pole" position (Africa relative to South America) calculated by *Cande et al.* [1988] (solid circle), the fossil transform's (suspended valley) pole, the poles calculated by *Minster and Jordan*, [1978] and *Searle et al.* [1994] (solid triangles). The 95% confidence level error ellipse is indicated.

positive topographic anomaly reaches a maximum value of about 500 m in a very limited area across the RTI in a transform with the age offset and the slip rate inferred for the Romanche (Figure 12a). A negative topographic anomaly should be produced in young crust near the RTI. The theoretically estimated topographic anomalies can be compared with observed anomaly shown in Plate 2 that reaches up to 4 km. It appears, therefore, that lateral heat conduction at the RTI may have contributed to the Romanche topographic anomaly but cannot possibly explain it by itself.

Frictional Shear Heating

Frictional heating can be significant in transform zones [*Lachenbruch and Sass*, 1980; *Chen*, 1988]. Shear or frictional heating can raise the temperature along the fault plane by as much as 200°C to 400°C in large offset, slow slipping transforms [*Chen*, 1988]. However, frictional heat can be produced only in the brittle, upper part of the lithosphere and cannot significantly raise the temperature of the upper mantle. Applying *Chen*'s [1988] model to the Romanche suggests that a topographic anomaly of as much as 200 m can be created by shear heating (Figure 12b). An anomaly of that size will be limited to a distance of <5 km from the transform and to a zone intermediate between the two RTIs, where the temperature-dependent brittle/ductile boundary lies deeper below the seafloor.

The combination of heat conduction from the RTI and shear

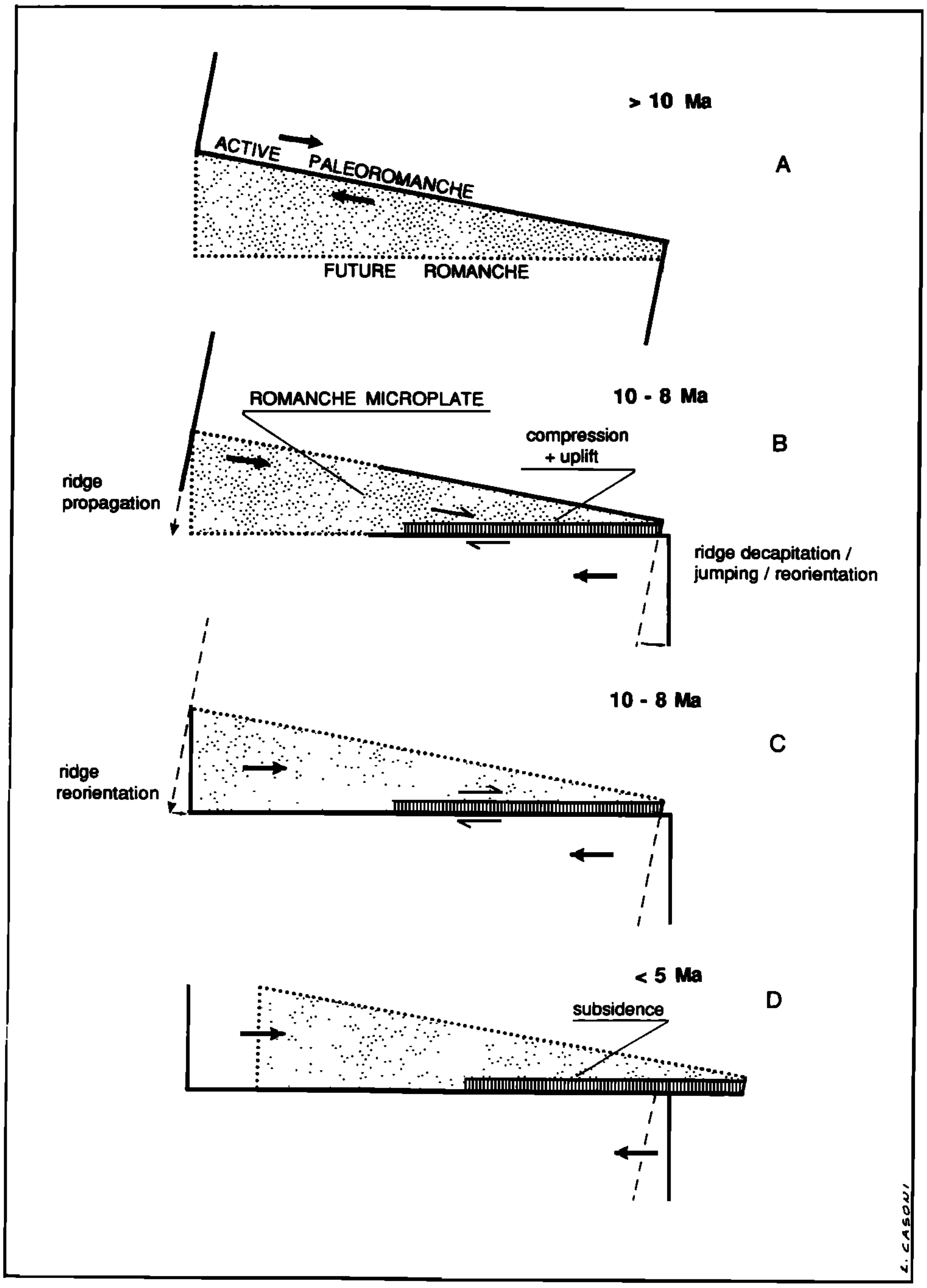

Figure 11. Schematic and simplified sequence illustrating the transition from a ridge/PaleoRomanche transform/ridge to a ridge/Romanche transform/ridge geometry. (a) The PaleoRomanche transform boundary is active before about 10 Ma. (b) and (c) Period of transition from the PaleoRomanche to the Romanche transform boundary, involving the formation of a temporary PaleoRomanche microplate, with migration and reorientation of the transform, ridge propagation, and reorientation at the western RTI and ridge decapitation, reorientation, and jumping at the eastern RTI. The possibility during the transition of oblique convergence of the old spreading direction with the new transform boundary could cause transpression and uplift of lithospheric slivers. (d) Present-day (<5 Ma) situation, with subsidence of the uplifted lithosphere.

frictional heating may cause a topographic anomaly of <1km in a transform such as the Romanche (Figure 12c). It appears, therefore, that uplift due to shear heating and thermal rejuvenation occurring when the old lithosphere moves close to the RTI cannot by itself explain a topographic anomaly that extends parallel to the transform for several hundred kilometers and reaches over 4 km above the predicted square-root-of-age level (Plate 2) and over 2 km above the adjacent "hot" MAR axis.

Lithospheric Flexure Due to Thermal Stresses

The hypothesis that thermal stresses due to lithospheric cooling and contraction with age may cause failure of the oceanic lithosphere and the formation of fracture zones has

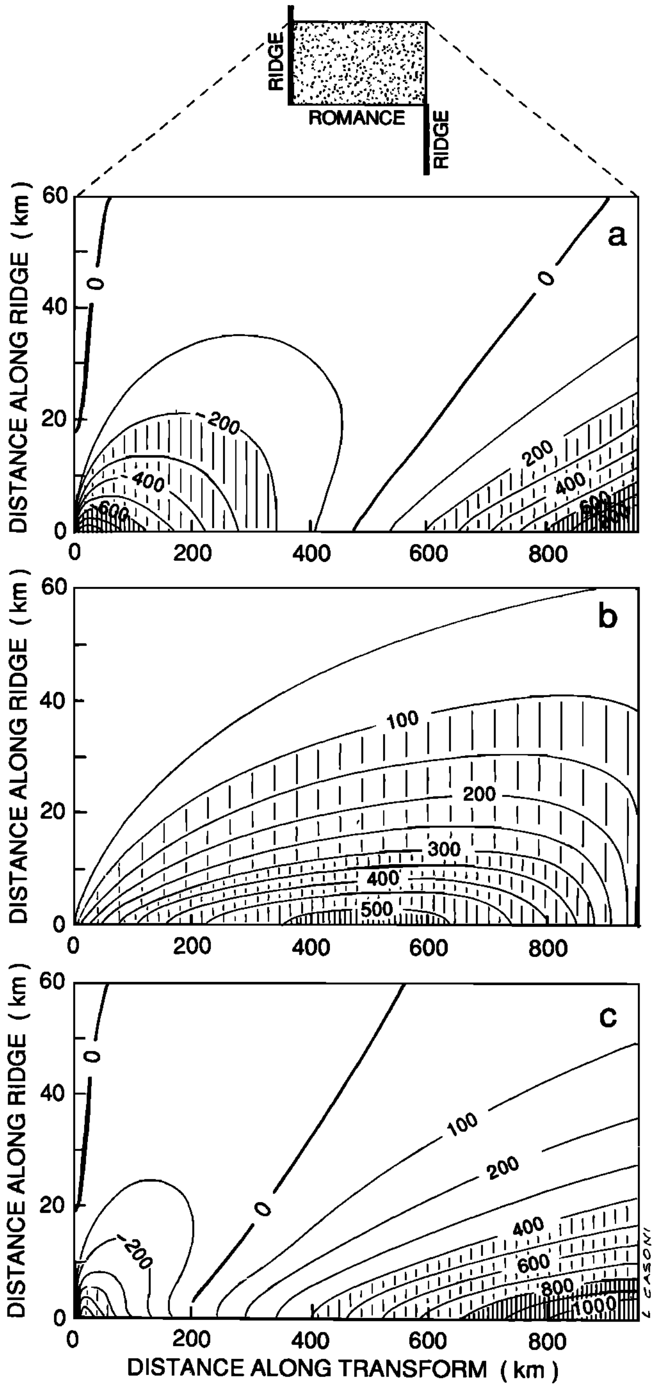

Figure 12. Topographic anomaly contour map for a transform with the characteristics of the Romanche (offset ~950 km and ~50 Ma) predicted by *Chen*'s [1988] thermal model. (a) Anomaly due to lateral heat conduction across the fault. (b) Anomaly due to shear heating along the fault. (c) Anomaly due to the two combined effects. The contour interval is 100 m for Figures 12a and 12c and is 50 m for Figure 12b.

been proposed by *Turcotte* [1974] and *Collette* [1974]. Whether thermal stresses are the prime cause of fracture zones remains unresolved; however, they may produce significant flexure of the lithosphere at fracture zones [*Sandwell and Schubert*, 1982; *Parmentier and Haxby*, 1986]. Models based on this hypothesis predict that tensional stresses develop at depth and compressional stresses develop near the surface of the brittle-elastic layer as it cools and thickens. The resulting bending moment causes the seafloor to flex downward near the transform, creating a peripheral topographic high that grows wider as the plate ages and thickens. *Parmentier and Haxby* [1986] have shown that for an age offset of 20 m.y. the positive topographic anomaly that develops on the old side of the transform due to thermal lithospheric flexure is <150 m. Although a somewhat larger anomaly can be predicted for the old plate across the Romanche RTI, it appears that lithospheric flexure due to thermal stresses cannot by itself contribute but a small fraction of the large topographic anomaly observed at the Romanche transform. However, lithospheric flexure could contribute significantly to the anomaly in a transpressional model of uplift.

Viscoelastic Deformation

Theoretical considerations have led to the hypothesis that nonlinear viscoelastic deformation of the lithosphere adjacent to a transform may lead to uplift and formation of transverse ridges on either side of the transform fault [*Bercovici* et al., 1992]. It is difficult to assess the extent to which this mechanism may account for the formation of the Romanche transverse ridge. According to *Bercovici et al.*'s theoretical formulation, an uplift of 4 km, as observed in the Romanche transverse ridge, would require a shear stress 1 order of magnitude above that necessary to modify rock behavior from viscoelastic to brittle [*Ranalli*, 1987]. Viscoelastic deformation along a transform would decrease with age of the lithosphere involved [*Bercovici et al.*, 1992]. This is contrary to the observation that the Romanche transverse ridge becomes prominent in old (>40 Ma) lithosphere. Moreover, viscoelastic forces tend to cause uplift on both sides of the transform, while the Romanche transverse ridge is prominent on the northern side but poorly developed on the southern side of the transform boundary. We infer that viscoelastic deformation may be important in some transforms but is not a major factor in the creation of the Romanche transverse ridge.

Hydration-Dehydration Reactions in Transform Zones

Hydration-dehydration of upper mantle peridotites can in principle cause significant topographic anomalies near an oceanic transform. Mantle-derived ultramafic rocks have been observed to lie at or close to the sea floor in the RTI inner corner of several low slip rate transforms. This is true also for both Romanche RTIs. Peridotites are likely in the presence of water to undergo hydration reactions whereby olivine and pyroxenes produce serpentine. Experimental work has shown that these reactions proceed at temperatures below 500°C [*Bowen and Tuttle*, 1949; *Seyfried and Dibble*, 1980]. Intense tectonization of the crust in a transform environment favors penetration of water at depth and may cause hydration of ultramafic rocks [*Bonatti*, 1976; *Francis*, 1981]. The subseafloor thermal structure of slow-slip transforms calls for deepening of isotherms away from the RTI and for their gradual rise when the old crust moves close to the hot ridge axis across the transform boundary (Figure 13). It is therefore likely that mantle-derived ultramafic rocks will undergo hydration during the first few million years after their emplacement near the RTI inner corner, to a depth below the seafloor increasing with age (distance from the RTI) and corresponding roughly to the 500°C isotherm. Dehydration reactions are likely to take place

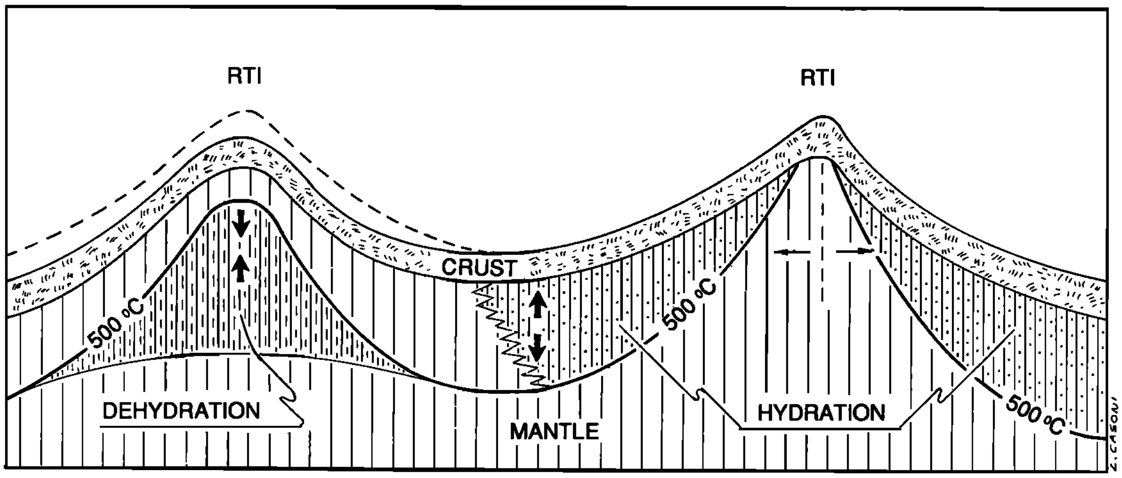

Figure 13. Model of hydration and dehydration of upper mantle peridotite in a slow-slip, long-offset transform (modified after *Rutter and Brodie* [1987]).

when the ultramafic rocks that underwent hydration near one RTI approach the other "hot" RTI located across the transform [*Rutter and Brodie*, 1987].

Dehydration reaction such as 5 serpentine = 6 olivine + 1 talc + 9 H_2O, start at about 450°C under PH_2O < Ptotal, or at about 500°C under PH_2O = Ptotal [*Rutter and Brodie*, 1987]. Reactions such as: 1 serpentine + 1 brucite = 2 olivine + 3 H_2O proceed at temperatures of 50°C to 80°C lower under similar pressure conditions [*Rutter and Brodie*, 1987; *Bowen and Tuttle*, 1949].

Assuming for simplicity that peridotite hydration occurs below 500°C and dehydration above 500°C, we can estimate roughly how deep below the seafloor the hydration front can reach and how thick the layer affected by dehydration will be in

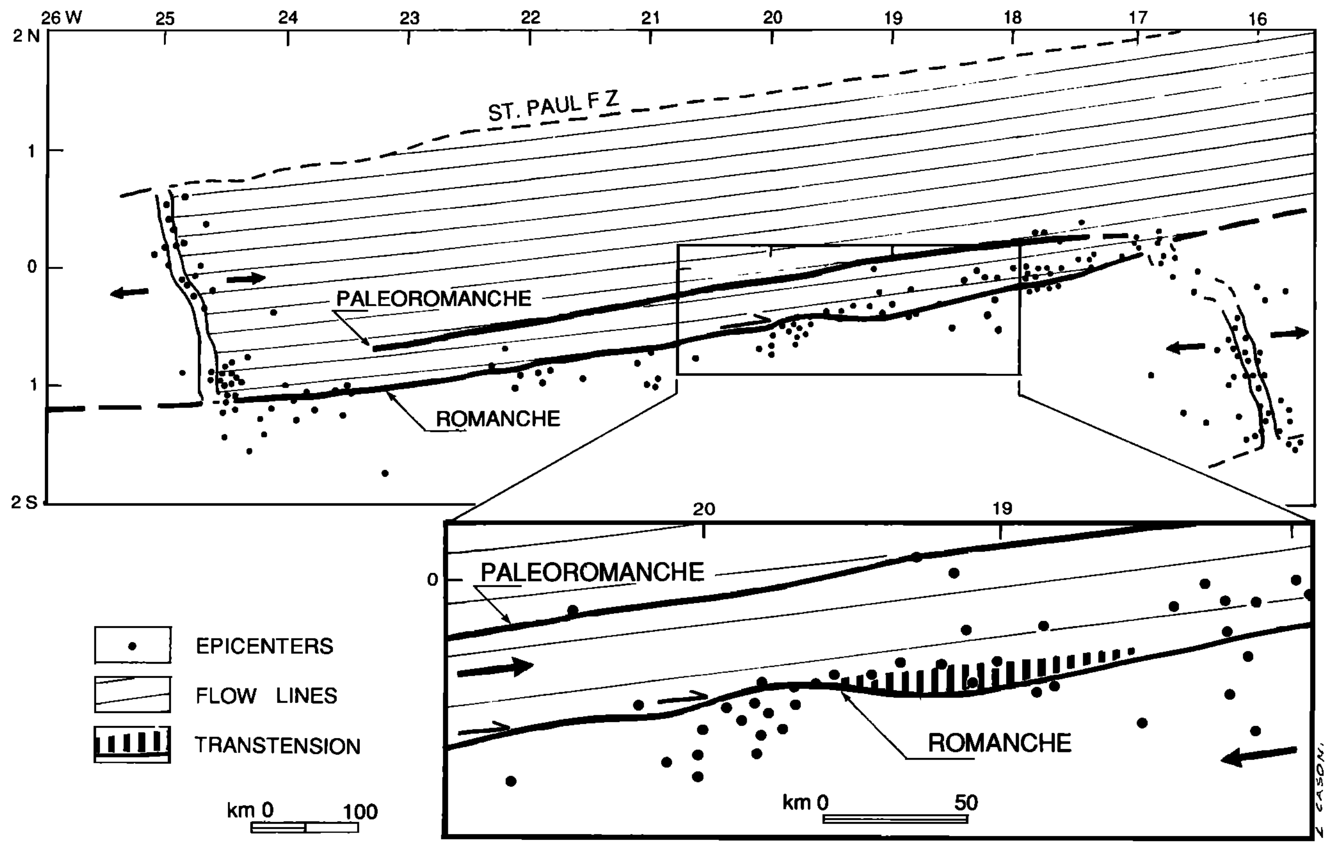

Figure 14. Trace of the presently active Romanche transform boundary and of the PaleoRomanche fossil transform versus inferred flow lines of motion of the lithosphere between Romanche and St. Paul drawn according to *Minster and Jordan* [1978] present-day plate motions. According to this model, old (30 Ma) lithosphere impacts obliquely (angle about 8°) against the eastern part of the transform boundary. Transpression may result. Transtension is likely along the transform boundary between 18°30' and 20°W, where in fact an ultradeep pull-apart basin is located.

a given transform (Figure 13). In a transform such as the Romanche, with an offset reaching over 40 Ma, the 500°C isotherm can sink deeper than 10 km below the seafloor. This will be the maximum depth of the hydration front. Assuming that the 500°C isotherm will rise as shallow as 4 km below the seafloor opposite to the hot RTI, a 6-km-thick layer may be affected by dehydration (Figure 13).

Hydration-dehydration reactions may result in significant changes in density and volume. Total serpentinization of a peridotite (with final H_2O content of about 15%) results in a change of density from an initial 3300 to about 2600 kg/m^3. Hydration/dehydration of ultramafic rocks may involve changes in volume [*Thayer*, 1966; *Hostetler et al.*, 1966; *MacDonald and Fyfe*, 1985; *O'Hanley*, 1992]. A 50% average degree of serpentinization affecting a 5-km-thick zone could result in a several hundred meters of uplift. This process could contribute significantly to the formation of transverse ridges in slow-slip transforms. Conversely, the dehydration of a 5-km-thick zone of 50% hydrated ultramafics would result in a several hundred meter subsidence. It appears therefore that upon approaching a RTI, the upper part of the lithosphere is subjected to two contrasting tendencies: thermal uplift and dehydration subsidence.

We conclude that although hydration-dehydration reactions can contribute significantly to vertical motions of lithospheric blocks near transforms, they cannot explain by themselves topographic anomalies that reach 4 km, as those observed in the Romanche region.

Longitudinal Flow of Melt

Longitudinal flow of melt beneath mid ocean-ridge segments may cause damming of melt against a cold transform boundary and formation of volcanic transverse ridges opposite a ridge/transform intersection [*Vogt and Johnson*, 1975]. This model would explain the location of the Romanche topographic anomaly opposite to the site of impingement of the MAR against the transform. However, a robust flow of melt below the MAR from the south is required. *Vogt and Johnson* [1975] suggested that an energetic longitudinal flow is likely when a hotspot discharges excess melt at or near a ridge axis. Even though a near-ridge hotspot may exist south of the Romanche FZ (i.e., the Ascension "hotspot"), two major MAR offsets are located between Ascension and the Romanche, i.e., the Chain and the Charcot FZs). They would dam northward flowing melt and protect the MAR/Romanche intersection from any excess melt. Relatively fresh basalt was sampled from the transverse ridge opposite to the MAR/transform intersection (station S13-07, Figure 4), suggesting that some volcanism may have taken place on the transverse ridge. However, the recovery of lower crustal gabbros and upper mantle peridotites at various levels from the slopes of the transverse ridge suggests that it is not a constructional volcanic edifice, but an uplifted sliver of upper lithosphere.

Vertical Movements Due to Transform-Related Transpression / Transtension

It has long been recognized that adjacent blocks in continental strike-slip faults can either converge or diverge, with important structural consequences including transpression and transtension [*Wilcox et al.*, 1973; *Christie-Blick and Biddle*, 1985]. Similar effects may occur in oceanic transforms [*Menard and Atwater*, 1967; *Bonatti*, 1978]. This is supported by the observation that a significant number of earthquakes occurring on oceanic transforms have a compressional or extensional mechanism [*Wolfe et al.*, 1993]. We suggest that transpression/ transtension related to oblique convergence of the moving lithospheric plate against the transform boundary is the major factor in explaining the anomalous topography observed at the Romanche. Oblique impacts may have occurred at different times due to (1) a nonstraight transform boundary both in the present-day Romanche or in the PaleoRomanche; (2) seafloor spreading flow directions that were nonparallel to the PaleoRomanche and/or to the present Romanche transform boundaries; and (3) transient convergence of the moving lithosphere relative to old and new transform boundaries during the transition from the old to the new transform/ridge geometry.

Nonstraight transform boundary. Topography, earthquake epicenters (Figure 1) and Seasat/Geosat gravity data (Plate 1) show that the orientation of the Romanche transform changes from a W-E direction in the western part to about WNW-ENE in the eastern part. This change in orientation does not appear to be gradual but to be the sum of changes occurring in a few discrete areas; the major of these is at about 19°-20°W; minor changes occur at 21°-22°W and 17°-18°W (Figure 14). Inferred flow-lines of lithospheric movement in the region between the Romanche and St. Paul FZs, drawn assuming *Minster and Jordan* [1978] present-day plate motions, strike 83°N (Figure 14). Figure 14 also shows the trend of the present-day active transform boundary as estimated by *Belderson et al.* [1984] and *Searle et al.* [1994] based on GLORIA data and the trend of the PaleoRomanche fossil transform, equated to the axis of the inactive valley.

Owing to the nonstraight transform boundary, portions of the lithospheric plate are likely to converge against portions of the transform boundary determining locally a transpressional regime (Figure 14). Conversely, extension may prevail in some other areas (Figure 14), possibly with a tendency for pull-apart basins to form. Earthquake epicenters (magnitude >3) for 1960/1990 are clustered in a few discrete areas (Plate 2 and Figure 14) suggesting that present-day tectonic activity is not distributed homogeneously along the Romanche transform but is concentrated in critical areas. For instance, a cluster of epicenters occurs between 19° and 20°W (Figure 14) where a major bend in the transform boundary is located. This geometry would imply areas of transtension close to the bend. The very deep (7.8 km below sea level) sediment-free basin observed in this portion of the Romanche transform valley at about 19°W [*Heezen et al.*, 1964] might be a pull-apart basin due to a local transtension regime. This deep pull-apart basin might have formed according to a mechanism similar to that suggested by *Crowell* [1974] to explain the Ridge Basin along the St. Andreas fault.

Nonparallel plate motion/transform boundary directions. The direction of motion of the lithospheric slab between the Romanche and the St. Paul FZs, estimated according to the method of *Minster and Jordan* [1978], indicates convergence by about 10° against the eastern portion (east of about 19°W) of the present-day Romanche transform boundary (Figure 14), implying a transpressional regime in this region. The topographic anomaly relative to the square root of age level on the northern side of the transform zone becomes large (>2 km) and continuous east of about 19°W

(Plate 2), that is, east of the 19°-20°W bend in orientation of the transform boundary. The anomaly extends eastward to beyond the RTI into the nonactive portion of the fracture zone. The convergence involving relatively old (>30 Ma), thick, and cold lithosphere is likely to trigger a compressional regime and to cause uplift according to a model outlined later. Opposite to the RTI, thermal rejuvenation would add an additional factor favoring uplift. Indeed, the topographic anomaly reaches its maximum (≃4 km) opposite the RTI (Figure 3).

Flow lines determined from *Cande et al.* [1988] stage pole 5-1 (time span from 9 Ma to present; F=60°N; l=39°W) appear, in general, to be nearly parallel to the present-day Romanche boundary, as well as to the PaleoRomanche (Figure 15). *Cande et al.*'s (1988) pole 6-5 (time span 19-9 Ma; F=59°07'N; l=37°26'W) would show a slight convergence with the central part of the PaleoRomanche boundary (Figure 15). It is remarkable that small differences (<5°) in the position of the pole of rotation can have strong effects as far as potential transpression or transtension along long-offset transforms such as the Romanche and the PaleoRomanche.

Oblique plate motion/transform directions during transition from old to new ridge-transform geometry. A non-instantaneous transition from the old to the new ridge-transform-ridge geometry (i.e., the migration from the PaleoRomanche to the Romanche transform boundaries and the formation of a temporary PaleoRomanche microplate) is likely to involve strong compressional or tensional stresses concentrated along the old and the new transform boundaries (Figure 11).

We suggest that compression due to the factors outlined above might have been, in a general way, the main cause of the anomalous uplifted lithosphere observed on the northeastern side of the Romanche. Compression has been documented by us on the easternmost peak (peak D) of the transverse ridge, where the thick sedimentary deposits are affected by folding and overthrusts (Figure 8). Compression has been inferred also along the eastward extension of the Romanche transform [*Lehner and Bakker*, 1983]. No clear evidence of compression was observed in our seismic reflection profiles from peaks A, B, and C. The reason could be that the transverse ridge near peaks A, B, and C is made of igneous oceanic crust. The small penetration of our sound source into igneous crust would prevent detection of compressional features, even if they were there.

We have evidence that the Romanche transverse ridge has been subsiding since at least 5 Ma. If the uplift was due mostly to a compressional regime, the 5 Ma to present subsidence suggests that compression ceased and was replaced by an extensional regime before that time. Evidence of extension roughly normal to the strike of the transform is provided by

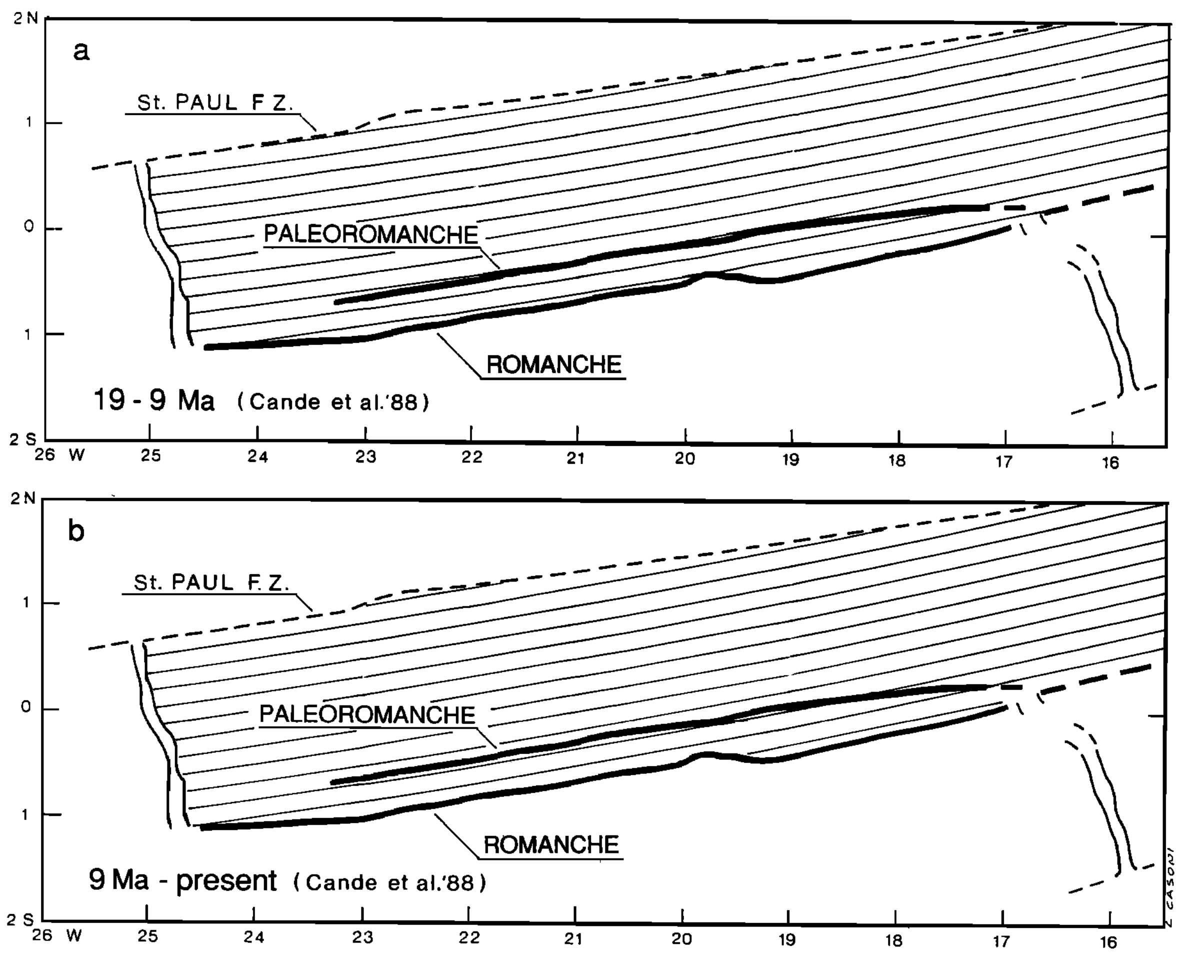

Figure 15. Traces of the present-day Romanche and of the inactive PaleoRomanche transform boundaries versus flow lines of motion of the lithosphere between the Romanche and St. Paul FZ. Flow lines are estimated from *Cande et al.* [1988]. (a) Stage pole 6-5 (19-9 Ma; (b) stage pole 5-1 (9 Ma to present).

seismic reflection profile ROM-3 (Figure 9). If we assume that the extensional features shown by profile ROM-3 are younger than about 5 Ma, we could then relate this extensional event to the subsidence of the transverse ridge. The shift from transpression and uplift to transtension and subsidence could be linked to the change in ridge-transform geometry. It may not be a coincidence that the subsidence of the anomalous transverse ridge appears to have started at about the time when a major rearrangement of the regional kinematic geometry must have occurred.

We have estimated that the transform boundary was located along the presently inactive PaleoRomanche valley up to about 8-10 Ma, because the valley disappears in 8-10 Ma crust (Figure 1 and Plate 2). A change in the direction of plate motion occurring between 10 and 8 Ma might have determined an unstable ridge-transform geometry, causing either a transpressional or a transtensional regime along the transform boundary. The unstable geometry might have caused the migration of the transform boundary to its present position. We can further speculate that in the area were the suspended valley (i.e., the old transform) merges with the presently active transform the tectonic regime changed to transtensional about 8 Ma. At the same time, peaks A, B, and C that at ~8 Ma were located close to the confluence of the old with the new transform, started to subside. Another event that probably occurred <8 Ma is the eastward jumping by about 80 km of the MAR axis at the eastern RTI to its present position. This ridge jumping increased the length of offset of the Romanche transform. It might be the last of a series of events that determined a considerable lengthening of the transform offset since the early stages in the opening of equatorial Atlantic.

Uplift Due to Transpression in a Transform/Fracture Zone

Let us consider a possible mechanism by which transpression in a transform/fracture zone might lead to crustal uplift. We assume a situation similar to that observed at the eastern end of the Romanche transform (Figure 16a), where an old, cold, thick lithosphere (elastic thickness H_o) converges against a young, thin, hot lithosphere (elastic thickness H_y). Compression is assumed to activate a thrust fault in the upper part of the old lithospheric plate, where δ is the dip of the fault and d is the maximum depth reached by the fault (Figure 16b). The fault plane may reactivate low- angle surfaces of weakness, such as the low-angle reflectors observed within the oceanic crust in various seismic reflection experiments [*McCarthy et*

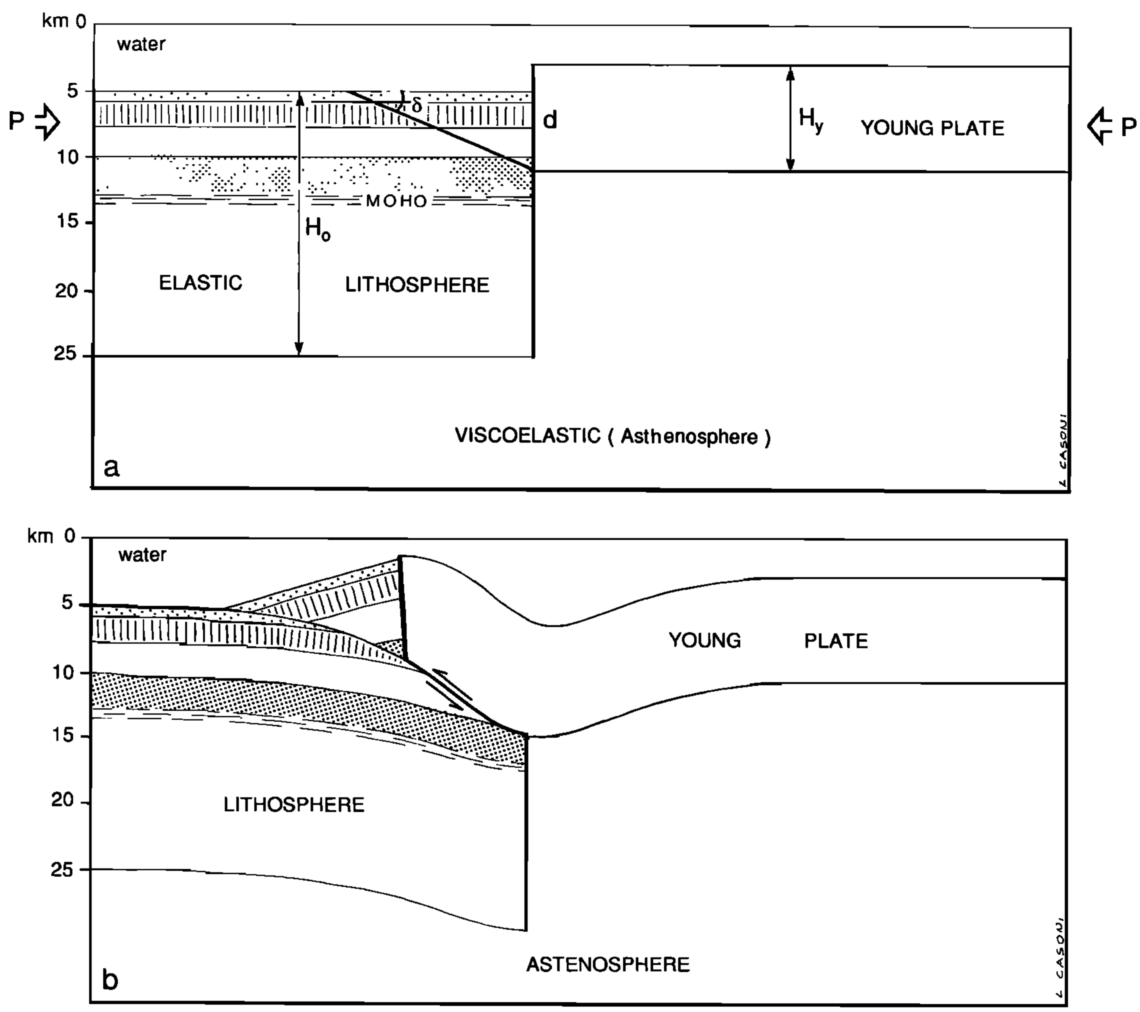

Figure 16. Model illustrating the effect of transpression across a transform in the vicinity of a RTI. (a) A young, thin lithosphere (thickness H_y) is in contact with old thick lithosphere (thickness H_o). A thrust fault is activated in the old plate. Dip of the fault is δ; maximum depth reached by fault is d. (b) Motion along the fault and flexure of the young plate may result from transpression.

al., 1988; *White et al.*, 1990; *Morris et al.*, 1993; *Salisbury and Keen*, 1993]. Moreover, lithospheric thermal flexure may facilitate thrust faulting. Earthquakes with reverse faulting mechanisms have been documented in the equatorial Atlantic transforms [*Wolfe et al.*, 1993].

In order to verify if the proposed model of compression can explain the topographic anomalies we observe at the Romanche, we have simplified the model of Figure 16a: the system lithosphere/astenosphere is modeled as an elastic plate (thickness H, Young's modulus E = 65 GPa, Poisson's modulus v = 0.25, density 3300 kg/m^3) overlying a viscoelastic half-space (density of 3300 kg/m^3 and rheology of a Maxwell solid with elastic constants similar to those of the elastic plate). The upper elastic layer is cut by a planar fault of infinite length in the direction normal to the plane of the drawning, with dip δ and maximum depth d (Figure 17). Deformation of the free surface (seafloor) is a response of the lithosphere/asthenosphere system to an instantaneous motion b along the fault plane. This deformation can be regarded as the sum of an instantaneous ("coseismic") elastic deformation and the deformation due to the "postseismic" relaxation of the stressed viscoelastic asthenosphere [*Rundle*, 1982]. A gravitational effect has to be included [*Rundle*, 1982]. Uplift due to thrusting along the fault has been estimated using equations by *Savage and Gu* [1985]. A dip of 20° has been assumed for the fault. This is an average value for the dip of the dipping reflectors [*Morris et al.*, 1993]. Assuming different elastic thicknesses of the lithosphere, we obtain the profiles shown in Figures 18a-18d. The theoretical profiles are compared with a N-S topographic profile across the fracture zone at peak C (Figure 19), and with the corresponding topographic anomaly. The maximum of the anomaly reaches about 4 km and is located 21-22 km from the trace of the transform. Comparison with the numerical models of Figure 18a-18d suggests that the observed uplift can be achieved when the entire younger plate overthrusts the old plate (Figure 18a, d = H = 8 km) and the motion along the fault is close to the width of the fault plane (b = 22 km; w = 3.96 km). If the depth of the fault is slightly less than the elastic thickness of the lithosphere (d < H), a smaller amount of motion along the fault is sufficient to achieve the same uplift (b = 13 km in Figure 18b and 15 km in Figure 18d). Moreover, a negative topographic anomaly is formed where x = 0; this negative anomaly may contribute to maintaining the transform valley.

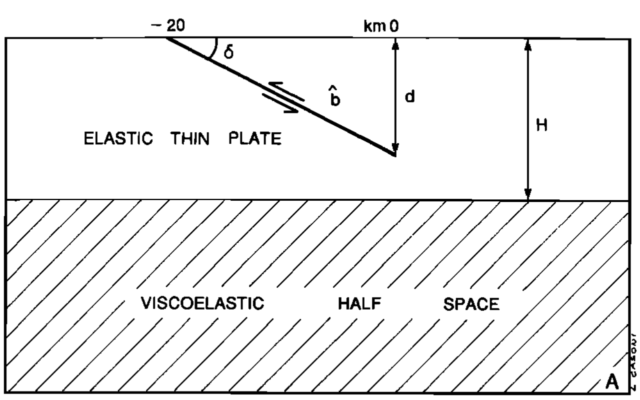

Figure 17. Simplified model of an elastic plate (thickness H; density 3300 kg/m^3, Young's modulus E=65 GPa, Poisson's modulus n=0.25) where a thrust fault is activated. Maximum depth of fault is d; dip of fault is δ. An instantaneous motion b is assumed along the fault plane. See text for explanation.

We note that a very large elastic lithospheric thickness does not allow an uplift as large as the observed uplift (if d = 8 km, H = 15 km, b = 22 km, w is 2.2 km; Figure 17). We also note that the equations used when d is not equal to H tend to exagerate the topographic depression around x = 0, if compared with more precise solutions [*Thatcher and Rundle*, 1984].

The model discussed above suggests that compression can cause the extent of crustal uplift inferred for the transverse ridge of the Romanche FZ. It is obvious, however, that these models are based on highly simplified assumptions and that an assessment of their physical reality has to wait for additional work.

Summary on Transform Migration and the Origin of the Tranverse Ridge

If we assume a steady state ridge-transform-ridge geometry and a one-way spreading rate of 1.75 cm/yr north of the transform, the uplift of the transverse ridge above the thermal contraction level must have started in lithosphere roughly 40 m.y. old and must have reached its maximum (above sea level) in lithosphere about 50 m.y. old, roughly opposite to the eastern RTI. This would give an average uplift rate of 0.3 mm/yr, compared to an average subsidence rate of 0.2 mm/yr from about 5 Ma to present. We have seen that the assumption of a steady state geometry is not strictly valid; however, we can safely assume a history of uplift that, with jolts and quiet periods, lasted for over 10 m.y. As a working hypothesis, we suggest that between 10 and 5 Ma we shifted from transpression/uplift to transtension/subsidence, although local zones of transpression/uplift may have been retained.

We reviewed the following potential causes: (1) lateral heat conduction; (2) shear heating; (3) hydration/dehydration of mantle ultramafics; (4) lithospheric flexure due to thermal contraction; (5) nonlinear viscoelastic deformation of the plate; and (6) igneous activity and volcanism.

We concluded that the above factors cannot explain the Romanche transverse ridge, although some of them (particularly lateral heat conduction) may have contributed to its formation to a small extent. The dominant factors are vertical tectonic motions due to transpressional and transtensional events related to nonstraight transform boundaries and to non-steady state ridge-transform-ridge geometries involving slight changes in the direction of spreading, ridge jumping and propagation, and transform migration.

An inactive former transform valley, identified north of the present transform boundary, gives evidence of transform migration. The PaleoRomanche transform boundary was probably located along this inactive valley up to about 8-10 Ma. Migration of the transform boundary to its present position was probably accompanied by creation of a transient Romanche microplate that changed its sense of motion (Figure 11). During the transition from the old to the new transform boundary, oblique convergence of moving lithospheric blocks against transform boundaries may have been particularly effective in creating transpressive stresses. Transform migration was probably followed by an eastward ridge axis jump. A transtension regime was established roughly 8-5 Ma near the eastern RTI, with subsidence of the transverse ridge and opening of small pull-apart basins, such as the ultradeep basin located along the transform valley between 18° and 19°W.

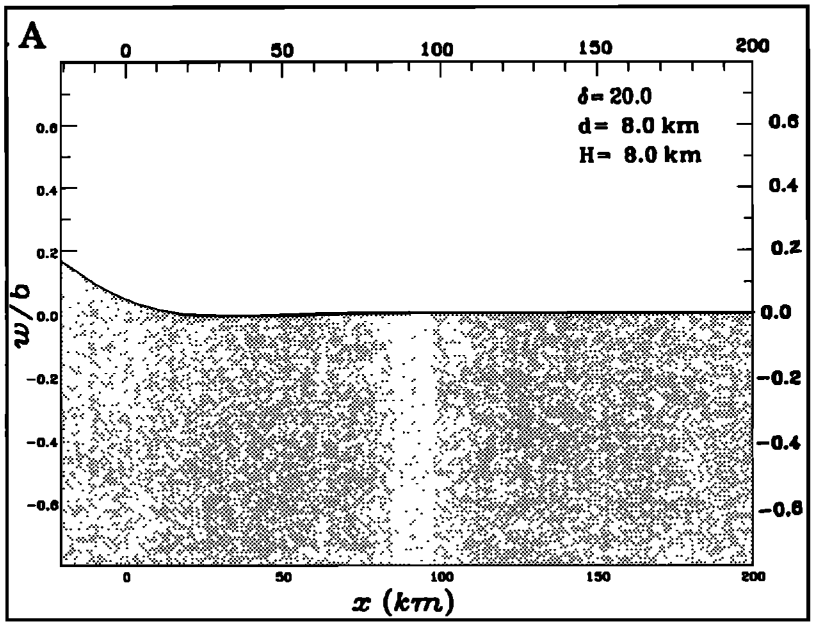

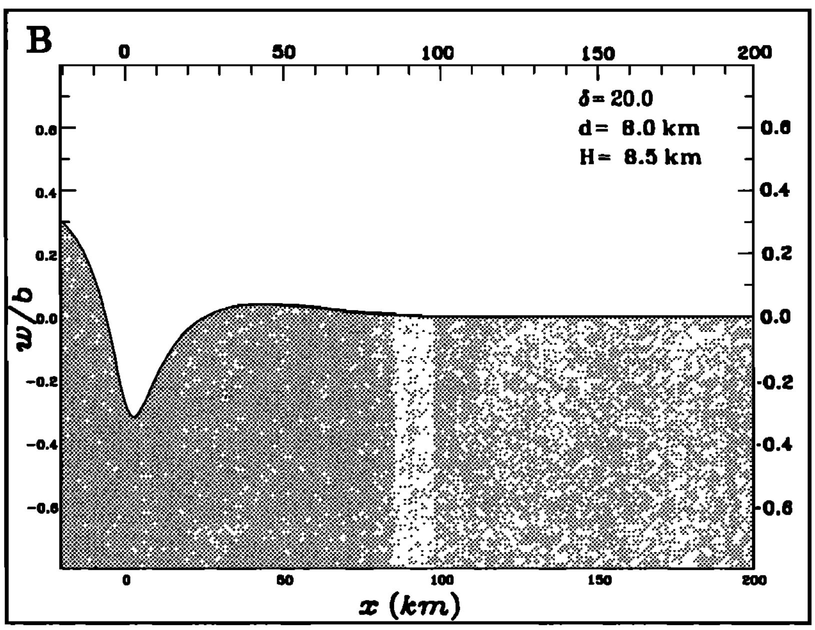

Figure 18. Predicted topographic profiles across a transform subjected to compression with activation of a thrust fault, according to the model of Figure 19. Different profiles are for different elastic thicknesses of the lithosphere. See text for explanation. These profiles should be compared with a N-S profile obtained across the Romanche FZ near peak C, shown in Figure 19.

General Conclusions

The present complex geotectonic situation on the eastern part of the Romanche transform and its complex evolution in time requires more field work before they are unraveled. An equally complex situation may be present at the western part of the transform. For instance, a major E-W aseismic valley, identified south of the active transform near the western RTI (Plate 2), may be a fossil transform boundary.

The different orientation of the western and eastern branches of the Romanche transform must cause a regional instability, which is enhanced by the convergence of the St. Paul FZ against the Romanche FZ in the African side. It is not surprising, therefore, that poles of rotation estimated from the eastern and western branches of the Romanche do not coincide with the poles of rotation describing the motion between North America and Africa and South America and Africa [*Belderson et al.*, 1984].

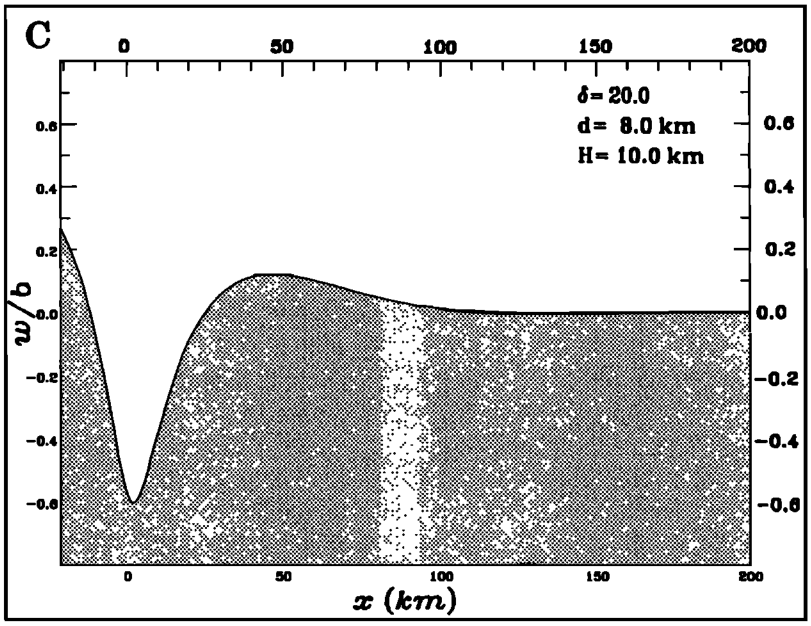

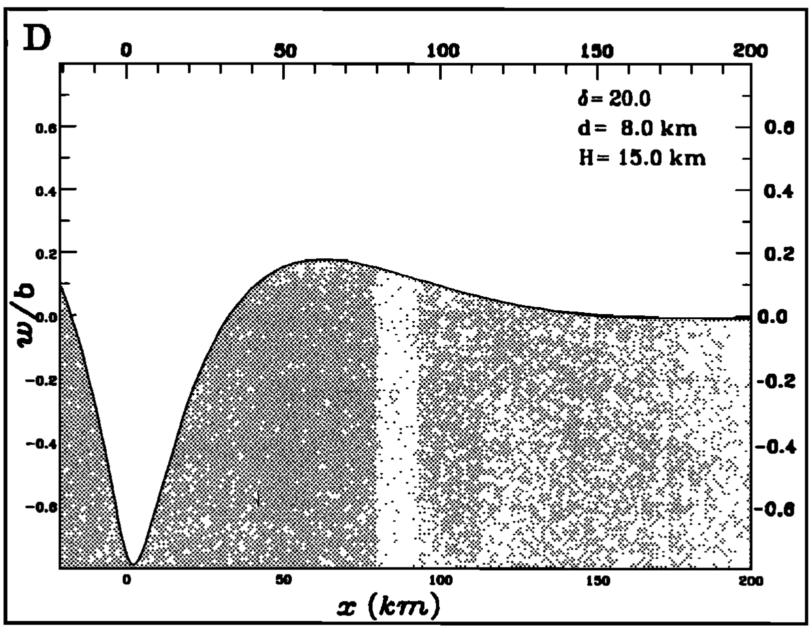

Figure 18. (continued)

The Romanche/PaleoRomanche transform system functioned throughout the evolution of the equatorial Atlantic and is and has been part of a broad equatorial megashear zone that includes the St. Paul FZ to the north and the Chain FZ to the south. In the equatorial zone (from roughly 3°N to 3°S) the cumulative length of transform offsets involving old, thick, cold, and rigid lithosphere is ~5 times the cumulative length of the ridge segments. Although the cumulative offset length was probably smaller in the past, this situation makes it very probable that transpressional and transtensional events occurred throughout the history of opening of the equatorial Atlantic, leading to intense vertical motions of lithospheric blocks and intermittent emersion of islands of tectonic origin. The transverse ridges bounding the equatorial transforms, resulting from such vertical motions, can be traced from one side of the Atlantic to the other. Drilling on one such transverse ridge on the South American margin (North Brazilian Ridge) ended at the base of a sediment pile in Eocene reef limestones [*Bader et al.*, 1970], suggesting that the transverse ridge was at sea level at that time.

The presence of elevated ridges and islands across the equator has probably had important consequences for deep cold water circulation between the South and the North Atlantic; for sedimentation both in terms of calcium carbonate dissolution (strongly affected by deep cold water circulation) and of transport of terrigenous matter; for faunal migrations, that might have been made possible to some extent by the presence of islands even after the separation of Africa from South America.

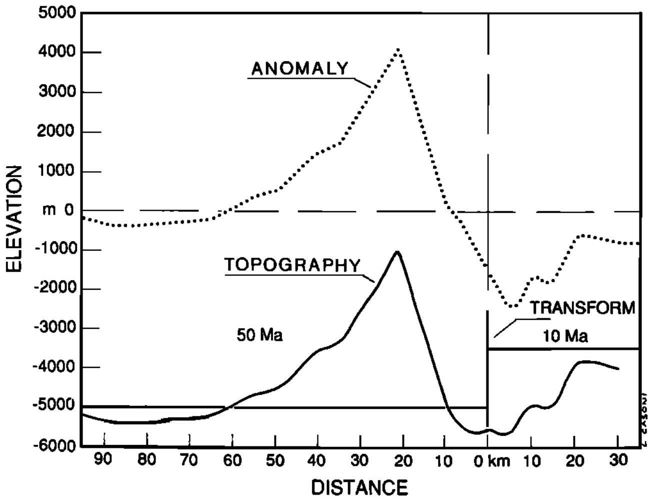

Figure 19. N-S topographic profile across the Romanche FZ at about 17°W near peak C. The dotted curve shows the topographic anomaly relative to the thermal contraction level predicted for 50 Ma and 10 Ma crust on opposite sides of the transform.

Acknowledgments. We are very grateful to Captain Leonid Sazonov and the officers and crew of the R/V *N.A. Strakhov* for their skill and cooperation in the field work. The Italian scientific group is particularly thankful for the warm hospitality extended to them on the ship. We are also grateful to A. Knipper, A. Praturlon, M. Zucchelli, B. D'Argenio, F. Frascari, P. Zucchini, G. Marozzi, L. Masini, L. Casoni, G. Zini, G. Gallerani, G. Carrara, F. Innocenti, and C. Casella, who in various capacities helped make the field work possible. We thank J.M. Auzende and R. Searle for providing us with unpublished bathymetric maps and D. Bercovici, H. Dick, and P. Wessel for constructive reviews of the manuscript. This research was sponsored in part by the Italian CNR (Progetto Strategico Mar Rosso/Dorsali). Contribution No. 5237 from Lamont-Doherty Earth Observatory.

References

Bader, R.G., et al., *Initial Reports of the Deep Sea Drilling Project*, vol. 4, pp. 59-67, U.S. Government Printing Office, Washington, D.C., 1970.

Belderson, R.H., E.J.W. Jones, M.A. Gorini, and N.H. Kenyon, A long range side scan (GLORIA) survey of the Romanche active transform in the equatorial Atlantic, *Mar. Geol., 56*, 65-78, 1984.

Bercovici, D., H.J.B. Dick, and T.P. Wagner, Nonlinear viscoelasticity and the formation of transverse ridges, *J. Geophys. Res., 97*, 14,195-14,206, 1992.

Bonatti, E., Serpentinite protrusions in the oceanic crust, *Earth Planet. Sci. Lett., 32*, 107-113, 1976.

Bonatti, E., Vertical tectonism in oceanic fracture zones, *Earth Planet. Sci. Lett., 37*, 369-379, 1978.

Bonatti, E., and A. Chermak, Formerly emerging crustal blocks in the equatorial Atlantic,*Tectonophysics, 72*, 165-180, 1981.

Bonatti, E., and K. Crane, Oscillatory spreading explanation of anomalously old uplifted crust near oceanic transforms, *Nature, 300*, 343-345, 1982.

Bonatti, E., A Chermak, and J. Honnorez, Tectonism and igneous emplacement of crust in oceanic transform zones, in *Deep Sea Drilling Results in the Atlantic Ocean: Ocean Crust, Maurice Ewing Ser.*, vol. 2, edited by M. Talwani et al., pp. 239-248, AGU, Washington, D.C., 1979a.

Bonatti, E., M. Sarntheim, A. Boersma, M. Gorini, and J. Honnorez, Neogene crustal emersion and subsidence at the Romanche fracture zone, equatorial Atlantic, *Earth Planet. Sci. Lett., 35*, 369-383, 1979b.

Bowen , N.L., and O.F. Tuttle, The system $MgO-SiO_2-H_2O$, *Geol. Soc. Am. Bull., 60*, 439-460, 1949.

Cande, S.C., J.L. LaBreque, and W.F. Haxby, Plate kinematics of the South Atlantic: Chron C34 to the present, *J. Geophys. Res., 93*, 13,479-13,492, 1988.

Chen, Y.J., Thermal model of oceanic transform faults, *J. Geophys. Res., 93*, 8839-8851, 1988.

Chermak, A., A structural study of the Romanche fracture zone based on geophysical data, M.S. thesis, 223 pp., Univ. of Miami, Miami, 1979.

Christie-Blick, N., and K.T. Biddle, Deformation and basin formation along strike-slip faults, in Strike-Slip Deformation, Basin Formation and Sedimentation, edited by K.T. Biddle and N. Christie Blick, *Spec. Publ. Soc. Econ. Paleontol. Mineral., 37*, 1-34, 1985.

Collette, B.J., Thermal contraction joints in a spreading seafloor as origin of fracture zones, *Nature, 251*, 299-300, 1974.

Crowell, J.C., Sedimentation along the San Andreas fault, California, in Modern and Ancient Geosynclinal Sedimentation, edited by R.H. Dott Jr. and R.H.Shaver,*Spec. Publ.Soc. Econ. Paleontol. and Mineral.*, 19, 292-303, 1974.

Forsyth, D.W., and B. Wilson, Three dimensional temperature structure of a ridge-transform-ridge system, *Earth Planet. Sci. Lett., 70*, 355-362, 1984.

Francis, T.G., Serpentinization faults and their role in the tectonics of slow spreading ridges, *J. Geophys. Res., 86*, 11,616-11,622, 1981.

Ginsburg, R.N., and N.P. James, Holocene carbonate sediments of continental shelves, in *The Geology of Continental Margins*, edited by C.A. Burk and C.L. Drake, pp. 137-155, Springer-Verlag, New York, 1974.

Gorini, M.A., The tectonic fabric of the equatorial Atlantic and adjoining continental margins: Gulf of Guinea to northeastern Brazil, Ph.D thesis, 116 pp., Columbia Univ., New York, 1977.

Haq, B.V., J. Hardenbol, and P.R. Vail, Mesozoic and Cenozoic chronostratigraphy and cycles of sea level change, in Sea Level Changes, An Integrated Approach, *Spec. Publ. Soc. Econ. Paleontol. Minerol., 42*, 71-95, 1988.

Haxby, W.F., Gravity Field of the World's Oceans, NOAA National Geophysical Data Center, Boulder Colo., 1987.

Heezen, B.C., E.T. Bunce, J.B. Hersey, and M. Tharp, Chain and Romanche fracture zones, equatorial Atlantic, *Deep Sea Res., 11*, 30-33, 1964.

Honnorez, J., J. Mascle, C. Basile, P. Tricart, M. Villeneuve, and H. Bertand, Margin of a segment of the Romanche fracture zone: A morphostructural analysis of a major transform fault of the equatorial Atlantic Ocean, *Geology, 19*, 795-798, 1991.

Hostetler P.B., R.G. Coleman, F.A. Mumpton, and B.W. Evans, Brucite in alpine serpentinites, *Am. Mineral., 51*, 75-98, 1966.

Karson, J.A., Lithosphere age, depth and structural complications resulting from migrating transform faults, *J. Geol. Soc. London, 143*, 785-788, 1986.

Lachenbruch, A.H., and J.H. Sass, Heat flow and energetics of the St. Andreas fault zone, *J. Geophys. Res., 85*, 6185-6223, 1980.

Langseth, M.G., and M.A. Hobart, Interpretation of heatflow measurement in the Vema fracture zone, *Geophys. Res. Lett., 3*, 241-244, 1976.

Lehner, P., and G. Bakker, Equatorial fracture zones of the Atlantic, in: Bally A.W. ed., Seismic expression of structural styles, *AAPG Stud. Geol., 15* (3), 25-29, 1983.

Louden, K.E., and D.W. Forsyth, Thermal conduction across fracture zones and gravitational edge effect, *J. Geophys. Res., 81*, 4869-4874, 1976.

MacDonald, K.C., Mid ocean ridges: Fine scale tectonics, volcanic and hydrothermal processes within the plate boundary zone, *Annu. Rev. Earth Planet. Sci., 10*, 155-190, 1982.

MacDonald, A.H., and W.F. Fyfe, Role of serpentinization in seafloor environments, *Tectonophysics, 116*, 113-135, 1985.

Mamaloukas-Frangoulis, V., Le zones de fracture oceaniques. L'example de Z.F. Vema et Romanche (ocean Atlantique), Ph.D. thesis, 288 pp., Univ. de Bretagne Occidentale, Brest, France, 1992.

McCarty, J., J.C. Mutter, J.L. Morton, N.H. Sleep, and G.A. Thompson, Relict magma chamber structures preserved within Mesozoic North Atlantic crust?, *Geol. Soc. Am. Bull.*, *100*, 1423-1436, 1988.

Menard, H.W., and T. Atwater, Changes in the direction of seafloor spreading, *Nature*, *219*, 463-467, 1967.

Minster, J.B., and T.H. Jordan, Present-day plate motions, *J. Geophys. Res.*, *83*, 5331-5354, 1978.

Monti, S., and H. Mercier, Carte bathymetrique de la zone de fracture de la Romanche (1/1000.000, SeaBeam EM12), IFREMER, Brest, France, 1991.

Morgan, J.P., and D.W. Forsyth, Three dimensional flow and temperature perturbations due to a trasform offset: Effects on oceanic crustal an upper mantle structure, *J. Geophys. Res.*, *93*, 2955-2966, 1988.

Morris, E., R.S. Detrick, T.A. Minshull, J.C. Mutter, R.S. White, W. Su, and P. Buhl, Seismic Structure of oceanic crust in the western North Atlantic., *J. Geophys. Res.*, *98*, 13,897-13,903, 1993.

O'Hanley, D.S., Solution of the volume problem in serpentinization, *Geology*, *20*, 705-708, 1992.

Parmentier, E.M., and W.F. Haxby, Thermal stresses in the oceanic lithosphere: Evidence from geoid anomalies at fracture zones, *J. Geophys. Res.*, *91*, 7193-7204, 1986.

Parsons, B., and J.G. Sclater, An analysis of the variation of ocean floor bathymetry and heat flow with age, *J. Geophys. Res.*, *82*, 803-827, 1977.

Ranalli, G., *Rheology of the Earth: Deformation and Flow Processes in Geophysics and Geodynamics*, 280 pp., Allen and Unwin, Boston, Mass., 1987.

Rundle, J.B., Viscoelastic-gravitational deformation by rectangular thrust fault in a layered Earth, *J. Geophys. Res.*, *87*, 7787-7796, 1982.

Rutter, E.H., and K.H. Brodie, On the mechanical properties of oceanic transform faults, *Ann. Tectonicae*, *1*, 87-96, 1987.

Salisbury, M.H., and C.E. Keen, Listric faults imaged in oceanic crust, *Geology*, *21*, 117-120, 1993.

Sandwell, D., and G. Schubert, Lithospheric flexure at fracture zones, *J. Geophys. Res.*, *87*, 4657-4667, 1982.

Savage, J.C., and G. Gu, A plate flexure approximation to postseismic and interseismic deformation., *J. Geophys. Res.*, *90*, 8570-8580, 1985.

Searle, R.C., The active part of the Charlie-Gibbs fracture zone: a study using sonar and other geophysical techniques, *J. Geophys. Res.*, *86*, 243-262, 1981.

Searle, R.C., M.V. Thomas, and E.J.W. Jones, Morphology and tectonics of the Romanche transform and its environs., *Mar. Geophys. Res.*, in press, 1994.

Seyfried, W.E., and W. Dibble, Seawater-peridotite interaction at 300°C and 500 bars: Implications for the origin of oceanic serpentinites, *Geochim. Cosmochim. Acta*, *44*, 309-321,1980.

Shackleton, N.J., and J.P. Kennet, Late Cenozoic oxigen and carbon isotopic changes at DSDP 284: Implications for glacial history of the northern hemisphere, *Initial Rep. Deep Sea Drilling Proj.*, *29*, 801-807, 1975.

Steckler, M.S., and A.B. Watts, Subsidence history and tectonic evolution of Atlantic-type continental margins, in *Dynamic of Passive Margins, Geodyn. Ser.*, vol. 6, edited by R. A. Scrutton, AGU, Washilngton, D.C., pp. 184-196, 1981.

Thayer, T.P., Serpentinization considered as a constant volume metasomatic process, *Am.Mineral.*, *51*, 685-710, 1966.

Thatcher, W., and J.B. Rundle, A viscoelastic coupling model for the cyclic deformation due to periodically repeated earthquakes at subduction zones, *J. Geophys. Res.*, *89*, 7631-7640, 1984.

Tucholke, B.E., and H. Shouten, Kane fracture zone, *Mar. Geophys. Res.*, *10*, 1-39, 1988.

Turcotte, D.L., Are transform faults thermal contraction cracks?, *J. Geophys. Res.*, *79*, 2573-2577, 1974.

Vail, P.R., and J. Hardenbol, Sea-level changes during the Tertiary, *Oceanus*, *22*, 71-79, 1979.

Van Andel, T.H., R.P. Von Herzen, and J.D. Philips, the Vema fracture zone and the tectonics of transverse shear zones in oceanic crustal plates, *Mar. Geophys. Res.*, *1*, 261-283, 1971.

Vogt, P.R., and G.L. Johnson, Transform faults and longitudinal flow below the mid-ocean ridge, *J. Geophys. Res.*, *80*, 1399-1428, 1975.

White, R.S., R.S. Detrick, J.C. Mutter, P. Buhl, T.A. Minshull, E. Morris, New seismic images of oceanic crustal structure, *Geology*, *18*, 462-465, 1990.

Wilcox, R.E., T.P. Harding, and D.R. Seely, Basic wrench tectonics, *Am. Assoc. Pet. Geol. Bull.*, *57*, 74-96, 1973.

Wolfe, C.J., E.A. Bergman, and S.C. Solomon, Oceanic transform earthquakes with unusual mechanisms or locations: Relation to fault geometry and state of stress in the adjacent lithosphere, *J. Geophys. Res.*, *98*, 16,187-16,211, 1993.

E. Bonatti, Lamont-Doherty Earth Observatory, Palisades, NY 10964 (e-mail: topy@ldeo.columbia.edu) and Istituto Geologia Marina, CNR, via P. Gobetti 101, Bologna, Italy.

Y. Chen, College of Oceanography, Oregon State University, Oceanographic Administration Building 103, Corvallis, OR 97331-5503. (e-mail: cheny@ucs.orst.edu)

L.Gasperini and M. Ligi, Istituto Geologia Marina, CNR, via P. Gobetti 101, Bologna, Italy.

A. Peyve and Y. Raznitsin, Geology Insitute, Russian Academy of Sciences, Moscow, Russia.

(Received March 8, 1993; revised April 25, 1994;
accepted April 29, 1994.)